DOI: 10.1002/ 17-04072-4

Article type: Progress Report

Key Trade-Offs Limiting the Performance of Organic Photovoltaics

Ivan Ramirez[1†], Martina Causa'[2], Yufei Zhong[2], Natalie Banerji[2] and Moritz Riede[1]**

[1]Clarendon Laboratory, Department of Physics, University of Oxford, Parks Road, OX1 3PU, Oxford, UK

[2]Department of Chemistry and Biochemistry, University of Bern, Freiestrasse 3, CH-3012, Switzerland.

[†]Present address: Heliatek GmbH, Treidlerstraße 3, 01139 Dresden, Germany

natalie.banerji@dcb.unibe.ch, moritz.riede@physics.ox.ac.uk

Keywords: bulk heterojunction blends, charge transfer states, ultrafast spectroscopy, organic donors, non-fullerene acceptors.

Abstract

2017 saw the publication of several new material systems that challenge the long-held notion that a driving force is necessary for efficient exciton dissociation in organic photovoltaics (OPVs) and that a loss of ~0.6eV between the energy of the charge transfer state E_{ct} and the energy corresponding to open circuit is general. In light of these developments, we combine insights from device physics and spectroscopy to review the two key performance trade-offs of OPV systems. These are the trade-off between the charge carrier generation efficiency and the achievable open circuit voltage (V_{oc}) and the trade-off between light absorption and fill-factor. The emergence of several competitive non-fullerene acceptors (NFAs) is exciting for both of these. We analyse what makes these materials compare favourably to fullerenes, including the potential role of molecular vibrations, and discuss both design criteria for new molecules and the achievable power conversion efficiencies.

1. Introduction

Although to some extent pushed into the background due to the emergence of perovskite solar cells, the organic photovoltaics (OPV) field, has made astounding progress both in fundamental understanding and device performance. In particular, new small molecule systems are increasingly challenging traditional paradigms of the field. Most exciting, non-fullerene acceptors (NFAs) bring into question the need for a driving force for charge transfer and consequently, previous empirical estimates of the achievable power conversion efficiencies. In this context, it is important to re-assess the origins and impact of recent key observations such as the increase in the electroluminescence yield in new OPV systems and the influence of molecular vibrations on non-radiative recombination. This progress report combines insights from the device and spectroscopy communities to provide an up-to-date perspective on the physics underlying the conventional and new systems and their performance limits.

The discussion is focused on two key issues, which have for long hindered OPV performances, and their applicability to the new systems. The first is a charge generation-open-circuit voltage (V_{oc}) trade-off, which has typically meant a driving force is required for charge transfer. Consequently, high performance devices have exhibited either a high short circuit current J_{sc} or a high V_{oc}.[1] The second is that the slow charge extraction and fast recombination mean optimum device performance is obtained at active layer thicknesses inferior to those required for full absorption. This is manifested in a trade-off between absorption and fill-factor (*FF*). We first provide a modern outlook on the physics behind these trade-offs. Both the fundamentals and their application to OPV systems are covered. We introduce the thermodynamics of photovoltaic conversion, which are currently the most powerful tool to describe the V_{oc} of OPVs. We cover the various theories behind charge generation and, to widen the debate, their implications on devices and especially their V_{oc}.

This leads us to consider the recent dilute and NFA systems and the exciting possibilities for experimental insights they offer. Some of these systems show record values for their emission yield and very low charge generation-V_{oc} trade-offs. Also, the role of non-radiative recombination due to molecular vibrations is receiving increasing attention. We examine the role of the trade-offs in limiting NFA performance and suggest potential explanations for their improved performance as well as some promising avenues for research.

2. Background

2.1: Photovoltaic conversion and V_{oc} losses

The current-voltage characteristics of any solar cell are depicted in **figure 1a)**. This '*JV'* curve is typically described by three quantities: the V_{oc}, the J_{sc} and, as a proxy for the maximum power, P_{max}, produced by the solar cell, the $FF = J_{sc}\,V_{oc}/P_{max}$. The power conversion efficiency (PCE), P_{max}/P , can then be calculated from these parameters, P_{in} being the sunlight power incident on the device. While J_{sc} and FF are relatively intuitive quantities linked to absorption and charge carrier extraction efficiency, the V_{oc} is conceptually more challenging. In OPV systems, low V_{oc} values compared to the theoretically achievable values represent a key performance loss and will be the focus of this perspective.

2.1.1 A thermodynamics perspective

To fully understand the V_{oc} losses and the various trade-offs for organic solar cells, it is essential to start from a thermodynamic description of solar cells in general, rather than from the often-used phenomenological description as a circuit or a *p-n* junction.[2–5] In this respect, it is convenient to use ideal solar cells and ideal conditions as a basis for the description of the performance losses in real devices.

At V_{oc}, when no current flows, an ideal semiconductor with bandgap E_g under ideal (monochromatic laser) illumination of exactly $FF = J_{sc} V_{oc} / P_{max}$ is governed by the simple reaction:

$$h\nu \rightleftharpoons e + h \quad (1)$$

in which the semiconductor absorbs photons, generating free charges that relax by re-emitting photons of energy E_g (radiative recombination). Because thermalisation of the excited electron (*e*) and hole (*h*) pairs can be neglected, this reaction is reversible and equilibrium is established. The presence of an energy gap implies that each additional *e-h* pair increases the chemical energy stored in the semiconductor by:[2]

$$\Delta U = \xi_n - q\Delta\phi + \xi_p + q\Delta\phi = \xi_n + \xi_p = E_{F,n} - E_{F,p} \quad (2)$$

where q is the elementary charge, $\Delta\phi$ the difference in electrical potential across the device, and $\xi_{n,p}$ are the chemical potentials of electrons and holes. In the language of physics, electrochemical potentials are expressed in terms of quasi-Fermi levels $E_{F,n}$ and $E_{F,p}$, for the electrons and holes, respectively. In devices, because the metal contacts are in equilibrium with the semiconductor, the external device bias $h\nu = E_g$ corresponds to the Fermi level splitting across the device $h\nu \rightleftharpoons e + h$:[5]

$$\Delta U = \xi_n - q\Delta\phi + \xi_p + q\Delta\phi = \xi_n + \xi_p = E_{F,n} - E_{F,p} \quad (3)$$

As a result, the voltage in the device corresponds to the chemical energy stored in the device and scales with the concentrations of the free electrons, *n*, and of the holes, *p*.

The equilibrium condition means that the rates at which *e-h* pairs are generated and annihilated (recombine) must balance. Since the rate at which *e-h* pairs recombine depends on *n* and *p*, generation and recombination dictate the number of charges in the device.

Mathematically, recombination and generation are represented by *R* and *G*, which are rates per volume. At equilibrium, for bimolecular *e-h* recombination:

$$\quad (4)$$

where β is the bimolecular recombination coefficient. A low coefficient increases the charge population and the energy in the device. However, q has a minimum value dictated by thermodynamics, and cannot be made arbitrarily small. A useful analogy to this situation, illustrated in **figure 1b)**, is that of a leaky bucket under the rain. If there are no leaks, the volume of water increases and fills the bucket, resulting in a higher gravitational potential energy. If there are leaks however, the bucket only partially fills and less energy is stored. The competition between the rate of the leak (size and number of holes) and rate of filling (amount of rain) determines the water level. Here, the rain represents the illumination, the water level the charge population and the leak their recombination, which, as we will discuss, can never be entirely avoided.

It is useful to note that [ ] describes the increase of $\Delta\phi$ compared to the intrinsic charge carrier concentrations in the dark $\xi_{n,p}$:

$$np = n_i^2 e^{\Delta E_F/k_B T} = n_i^2 e^{qV_{ext}/k_B T} \qquad (5)$$

with [ ] being the Boltzmann factor (k_B is the Boltzmann constant and T the temperature). In addition to voltage, the change in electrochemical potential also dictates the flow of current. It is therefore possible to derive the *JV* curve from thermodynamics. The simplest way is to integrate *G* and *R* over the semiconductor thickness to obtain the absorbed and emitted photon fluxes $j_{|\ \ |}$ and V_{ext}.[3] The difference in those fluxes corresponds to the current of *e*-*h* pairs coming out of the device:

[ ] (6)

Combining this with equations (5) and (4), the device's *JV* curve under illumination is obtained without reference to *p*-*n* junctions or electrical models:

$$J(V) = q \qquad (7a)$$

Equation **(**7a**)** can then be rewritten as:

$$J = J_0\left(e^{\frac{qV}{k_BT}} - 1\right) + J_{photo} \qquad (7b)$$

where J_{photo} is the photo-generated current and J_0 is the dark current, an important quantity, which corresponds to thermally generated charges .

It is useful to expand the quantities describing the *JV* curve in the context of thermodynamics. The short circuit current density J_{sc} is the current density extracted without any load (V = 0) and can theoretically reach $qj_{abs.}$ The maximum fill factor *FF* is dictated by thermodynamics and cannot exceed 0.89.[3] Graphically, it corresponds to the area ratio of the dark and light rectangles in **figure 1a)**. V_{OC} is the point at which no current flows. For a *JV* curve under illumination it corresponds to the maximum 'electrochemical' or 'free' energy ΔE_F that can be extracted per *e-h* pair. Solving the *JV* equation (7b) for *J=0*:

(8)

or, by using equation **(4)** and Boltzmann statistics:

$$qV_{oc} \approx E_g + k_BTln\left(\frac{np}{N_cN_v}\right) \qquad (9)$$

where N_c and N_v are effective densities of states in the conduction and valence band (constants) and the second term must be negative. Even for a perfect semiconductor, qV_{oc} must be lower than E_g.[6] This is because equation **(4)** also holds in the dark, when charges are thermally generated. This sets the value of β and therefore of np.

2.1.2 Shockley-Queisser limit and heat

The sun is of course not a laser emitting photons at a single energy E_g. As a result, losses via sub-gap transmission and thermalisation occur. *e-h* pairs created by photons with $hv > E_g$ rapidly thermalise and lose excess energy as heat. As traditional solar cells only harvest the chemical energy of *e-h* pairs, this heat represents an unavoidable loss and V_{oc} is dictated by E_g

instead of the absorbed photon energy. Light with energy $h\nu < E_g$, on the other hand, is not absorbed. Most solar photons are in the near infrared (IR) but more energy is wasted as heat with a semiconductors having a lower E_g. Thus, a compromise must be made when choosing E_g for best solar cell performance. In the ideal case, all recombination is radiative, all photons with $h\nu > E_g$ are absorbed and the charge carrier mobility is infinite. This is known as the Shockley-Queisser (SQ) limit. With this ansatz, the ideal and theoretical maximum V_{oc}^{SQ} can be calculated from equation (8). The resulting minimum achievable V_{oc} loss $qV_{ext} = E_{F,n} - E_{F,p} = \Delta E_F$ depends on [illegible] and T. Including the thermalisation heat loss, the best PCE according to SQ is therefore ~32% for a single junction (with one E_g) under one sun illumination, instead of the absolute thermodynamic limit of ~85%.[3] To approach the absolute thermodynamic limit within the SQ framework, multiple junctions (many E_gs) can be used. For an infinite number of gaps, the thermalisation loss is entirely avoided and, in the presence of solar concentration, the 85% limit is recovered. As a side note, thermalisation does not affect the thermodynamic treatment as the system remains approximately in equilibrium.

2.1.3 Origin of V_{oc} losses

While thermalisation constitutes a largely unavoidable heat loss, there exists a significant source of avoidable heat loss. This is non-radiative recombination, which occurs through electron-nuclear (vibronic) coupling and represents an additional leak in our bucket analogy. Instead of being emitted as a photon of energy E_g, the *e-h* pair energy is dissipated as nuclear excitations (vibronic quanta known as phonons). These typically have much lower energies than the semiconductor gap. As a result, non-radiative recombination is often inefficient because energy conservation requires many phonons to be emitted simultaneously. Roughly, the rate of non-radiative recombination [illegible] decreases exponentially with the number of quanta

required for recombination. This is the gap law, which is most commonly discussed for isolated organic molecules. However, it is also relevant to semiconductors. As has been discussed in the context of hybrid organic-inorganic perovskites, it explain why traps constitute efficient recombination centres.[7] Since these are lower in energy, fewer phonons are required.

For organic semiconductors, nuclear vibrational energies β are very high (~160meV vs 16.5meV for perovskites).[8,9] Since the number of quanta needed for non-radiative recombination scales as $\frac{\Delta E_F}{\beta}$, these high vibrational energies have recently been found to cause efficient non-radiative recombination in OPV systems, even in the absence of traps.[9] The high-energy 160meV mode is assigned to unavoidable C-C vibrations and is understood to be one of the key factors limiting the PCE of OPVs. The extent to which this mode is unavoidable is discussed in depth in section 6, but we briefly introduce the relevant molecular physics here.

The nuclear potential landscape as a function of inter-atomic distance is illustrated for a molecule in **figure 2**. Since there are many atoms that can move, distances are typically described as an effective coordinate Q_m corresponding to possible vibrational modes of nuclei. These motions are associated with a characteristic energy β and, because of the gap law, only the high energy vibrational modes are relevant. In the Born-Oppenheimer approximation, the nuclear and electronic motions can be treated independently. Then, k_{nr} is given by Fermi's golden rule and is proportional to the overlap of the nuclear (vibrational) wavefunctions ΔE_F in the electronic excited-state (*exc*) and ground-state (*GS*). This is the Franck-Condon factor:

$$k_{nr} \propto \left| \int \chi_{exc}^{*} \chi_{GS} \, dQ_m \right|^2 \qquad (10)$$

The wavefunction overlap decreases exponentially with the number of quanta separating the nuclear states between the excited and ground electronic levels, which is the origin of the gap law. As illustrated in **figure 2**, crossing from one electronic level to another typically requires

overlap between nuclear modes with very different vibronic quanta (see curved arrow in **figure 2**, going from vibrational level 0 in S_1 to 5 in S_0) and it is accordingly inefficient. A common misconception is that recombination corresponds primarily to a loss in (short-circuit) current. In fact, non-radiative recombination primarily corresponds to a loss in free energy (voltage). In general, the fraction of charges that recombine radiatively is determined by the competition between k_{nr} and the emission rate, and can be expressed by either the photoluminescence quantum efficiency (PLQE) or the electroluminescence quantum efficiency (EQE_{EL}). The impact of non-radiative recombination on V_{oc} can be derived from detailed balance and is given by:[4,10]

$$np \qquad (11)$$

The derivation is based on a system with an imperfect external quantum efficiency (*EQE*), which is the yield of extracted *e-h* pairs compared to incident photons. The internal quantum efficiency *IQE* corresponds to the yield of extracted *e-h* pairs from photons absorbed in the active layer. Of course, a high k_{nr} also reduces *np* and with that V_{oc}. A radiative trap for example, would reduce only *np*, while a non-radiative one would reduce *np* by the same amount and further decrease the voltage through the loss in emission. As a side note, the reason we consider k_{nr} to conceptually constitute a voltage and not a current loss, is that the effect of a faster k_{nr} on J_{sc} can always be mitigated by a faster charge extraction.

2.2 Organic Photovoltaics

2.2.1 Organic semiconductors

Organic semiconductors are solid-state assemblies of conjugated polymers or small molecules weakly coupled by van der Waals forces. Because of this weak coupling, only a moderate energetic splitting occurs in the solids. This is unlike atomic semiconductors, for which energy level splitting is strong and bands are fully delocalised. Instead, ordered molecular

crystals display narrow bands. In films, the disorder induced by the many possible electronic and geometrical conformations of the molecules strongly localises states. As a result, the solid's properties lie somewhere in-between those of isolated molecules and (moderately) delocalised semiconductors, but typically closer to the former.

The poor screening of charges in organic semiconductors means that the ionised energy levels are substantially distinct from the neutral levels and that two gaps (optical and electrical) co-exist in the solid. When absorbing light, organic semiconductors therefore show a fundamentally different behaviour to textbook inorganic semiconductors. This is illustrated in **figure 3**, which depicts the optical and electrical (*e*-*h*) gaps for various levels of delocalisation. The optical gap [ ] is defined by the S_0-S_1 transition (between the electronic ground and first excited state), and the electrical gap $n_i = p_i$ is given by:

$$np = n_i^2 e^{\Delta E_F / k_B T} = n_i^2 e^{q V_{ext} / k_B T} \quad (12)$$

where [ ] and EA are the ionisation potential and electron affinity of the organic semiconductor film, M^+ and M^- the energies of isolated charged molecules, and the polarisation energies $P_i \sim$ 1eV correspond to the partial screening of charges by the solid medium.[11] The neutral (optical states) are excitons, so that the optical and electrical gaps differ by the exciton binding energy. In perfect crystals, the regular couplings between molecules imply that excitons are somewhat free to travel (narrow band formation). However, energetic and positional disorder typically results in highly localized states akin to those of individual molecules. That being said, whether the primary photo-excitations in conjugated polymers (with potential intrachain delocalization) are free charges in energy bands that eventually localize to excitons or whether excitons are directly generated, has been debated.[12–14] For highly ordered systems, such as polydiacetylene quantum wires, delocalized excited states with quantum coherence lengths reaching tens of micrometres have indeed been observed.[15] There is also experimental and theoretical evidence of enhanced

excited-state delocalization on the sub-100 fs time scale following light absorption, allowing ultrafast coherent processes.[16–22] Nevertheless, the consensus is nowadays that both solution-processed and vacuum deposited organic semiconductors are excitonic in nature at the level of disorder and timescales most relevant to OPV operation.

2.2.2 Donor-acceptor heterojunctions

The energy required to split excitons $k_B T$, is much larger than the thermal or electrical energy available at solar cell operating conditions. This results in very low photo-currents and efficiencies for neat materials. It is possible to circumvent this problem by employing two materials with carefully chosen energy levels, such that at an interface between the materials, or 'heterojunction' (HJ), neutral excitations are split. Electrons end up on one of the materials, the electron 'acceptor' (A), after being donated by the other, donor, material, (D). The reverse process (hole transfer) also occurs (e.g. ref. [23]), but historically most absorption has taken place via the donor, so that electron transfer has received almost all of the attention. A physically entirely incorrect,[24] but illustrative schematic is provided in **figure 4a)**. A first issue with the diagram is that it is not possible to satisfactorily depict excitons and charges together on it. A second, as will be discussed in detail, is that the relevant energetics at the HJ are not those of the bulk. Nonetheless, while the schematic should not be over interpreted or used in detailed discussions, it does introduce the concepts of hole and electron transfer. In the ideal case, the electrical gap at the D-A junction k_B should match the smaller one of the optical gaps $E_{g,opt}$ of D or A:

T (13)

such that V_{oc} can be maximised. However, in practice, optimal device performance has been obtained with j ,[25,26] which induces a free-energy (V_{oc}) loss. Consequently, charge generation (a 'two step' process) has been thought to require an energetic driving force to

overcome the exciton's Coulomb separation barrier. Taking r_{ex} as the exciton radius and ϵ_0, ϵ_r as the vacuum and relative permittivities, this barrier can naively be estimated to be

 and is extremely large (300-500 meV).[27,28] For many systems, charge transfer at D-A heterojunctions is extremely efficient,[29] provided excitons reach it. The low exciton diffusion length compared to the absorption length of ~100 nm implies that a simple stacking of the donor and acceptor into a 'planar heterojunction' (PHJ, **figure 4c)**) yields low currents. Either, not all of the light is absorbed, or excitons recombine before reaching the D-A interface. Instead, the paradigm has been to blend the materials into a 'bulk heterojunction' (BHJ, **figure 4d)**) in volume rations typically between 1:1 and 1:4.

For the polymer:fullerene BHJs with the highest photo-currents (~20 mA cm^{-2}), EQEs greater than 80% are obtained across the spectrum,[30] with IQEs on par with those of the best perovskite devices, albeit at the cost of a low V_{oc}. In general, the EQE of an OPV system can be written as a product:

$$\boldsymbol{j}_{em}(\boldsymbol{V}) \qquad (14)$$

of the absorption  , the exciton collection at an interface  , the exciton dissociation at the interface η_{Diss}, and the charge collection  probabilities. The BHJ architecture improves the  term, but negatively impacts  and introduces several challenges. These include a high internal interfacial area between D and A, at which recombination can occur, a critical dependence of performance on optimised domain size, and a poor charge transport relative to neat materials.

2.2.3 Small molecules and polymers

An important point to bear in mind is that there are several OPV sub-technologies. Research has overwhelmingly focused on solution-processed polymer:fullerene blends and acceptors have almost exclusively consisted of fullerenes and their derivatives. More recently, soluble

small molecules and oligomers have received increasing attention as donors and now especially as acceptor alternatives to fullerenes.

Important materials used with solution processable fullerenes have included polythiophenes such as regioregular poly(3-hexylthiolphene) (P3HT), where a favourable morphology was obtained by thermal annealing,[31] and for which PCEs of up to 6.5% were demonstrated.[32] Related polythiophenes, such as poly(2,5-bis(3-hexadecyl-thiophen-2-yl)thieno[3,2-*b*]thiophene (pBTTT) show highly ordered, semicrystalline chain packing and are therefore excellent model systems for photophysical studies.[33–36] The need for higher PCE has pushed the OPV field towards the development of push-pull copolymers (also known as 'D-A' copolymers, which can introduce confusion). These consist of alternating electron-donating and electron-withdrawing moieties along their backbone, yielding a tuneable bandgap and improved absorption in the near-infrared part of the solar spectrum compared to homopolymers. Noteworthy is the PTB series of polymers, composed of thieno[3,4-*b*]thiophene and benzodithiophene moieties (such as PTB7-Th also called PCE10 with 10% efficiency),[37–39] or poly[(5,6-difluoro-2,1,3-benzothiadiazol-4,7-diyl)-*alt*-(3,3‴-di(2-octyldodecyl)-2,2′;5′,2″;5″,2‴-quaterthiophen-5,5‴-diyl)], having 11% efficiency and known as PCE11.[40] Important drawbacks of the push-pull copolymers include their complex synthesis, elaborate processing, and challenging photophysics due to enhanced localization in the excited state.[37] Common fullerene acceptors include C_{60}, [6,6]-phenyl-C61-butyric acid methyl ester ($PC_{60}BM$), [6,6]-Phenyl-C71-butyric acid methyl ester ($PC_{70}BM$ with slightly enhanced visible absorption) and the indene-C_{60} bis-adduct ICBA.

Small molecules have the inherent advantage over polymers that their synthesis is better defined (fixed molecular weight) and their purification is more straightforward. This can for example avoid traps caused by homo-couplings (imperfect push-pull alternations).[41,42] Many small molecules can furthermore be sublimed under vacuum, which can be used both to obtain highly pure starting materials, or as an alternative to solution-processing for device

fabrication. Vacuum deposition has historically been the method of choice for all small molecule solar cells. Here, phthalocyanines have played a similar role to P3HT for polymers,[43–45] Their replacement by push-pull molecules has resulted in BHJ PCEs beyond 9.5%.[46–49] More recently, solution-processed oligomers such as 7,7′-(4,4-bis(2-ethylhexyl)-4*H*-silolo[3,2-*b*:4,5-*b*′]dithiophene-2,6-diyl)bis(6-fluoro-4-(5′-hexyl-[2,2′-bithiophene]-5-yl)benzo[*c*][1,2,5]thiadiazole) (p-DTS(FBTTh$_2$)$_2$, have also achieved high efficiencies through favourable self-assembly with fullerene acceptors.[50] Lastly, solution-processable small molecules represent the most successful non-fullerene acceptors (NFAs) to date: Over 13% efficiency has been achieved in single junction polymer blends with NFAs, which we will further discuss in section 6.[51]

Compared to solution processing, the advantages of vacuum thermal deposition are reproducibility, avoidance of (typically harmful) solvents, easy access to multilayer structures, compatibility with surface characterisation techniques and, from the success of organic light-emitting diodes (OLEDs), a proven scalability. Its main disadvantage is a high initial cost for the equipment, which has largely contributed to the dominance of solution processing at research scales. At commercial scales, slot-die coating offers the lowest processing costs but vacuum deposition is more suitable to the production of multi-junction devices.[43]

The reason we emphasize these different material classes and processing routes is that their underlying physics is different. For example, polymers can exhibit high delocalisation along chains but are typically less crystalline than small molecules, and film growth proceeds entirely differently between vacuum deposition and solution processing.

2.2.4 Charge transfer states

Following the pioneering work of Vandewal *et al*., it is widely accepted that for OPV systems with fullerene acceptors, recombination and some or all of charge separation occur via an intermediate ‘charge transfer’ (CT) state.[25,52–54] A populated CT state can conceptually be

thought of as a bound *e-h* pair exciton residing across a donor-acceptor HJ (**figure 4b)**). To avoid confusion with the singlet excitons formed by light absorption in D or A, we will nevertheless refrain from calling the CT state an exciton in this report. CT states are coupled to the ground state and can therefore be studied by absorption, electroluminescence (EL) or photoluminescence (PL) spectroscopy. However, their very low oscillator strengths mean that specialized techniques, such as photo-thermal deflection spectroscopy, are required for absorption measurements. CT states can also yield free charges upon direct excitation, which implies that they can also be studied with sensitive spectrally-resolved current measurements, including Fourier-transform spectroscopy and dedicated sensitive EQE set-ups. The CT state IQE is however much debated and discussed further on.[55–58]

CT state absorption typically appears as a broad sub-gap Gaussian band,[52] although for some systems, vibronic progressions are resolved.[59] The broad Gaussian is understood as resulting from disorder and molecular reorganisation due to the presence of partially screened charges on the donor and acceptor, with a potential slow reorganisation of the environment in response to the presence of an interfacial dipole,[54,59] and a contribution from disorder.[60] As a result, the CT absorption ( ) spectrum is typically fitted according to Marcus theory with:

$$\alpha_{ct}(E,T) \propto f_0 exp\left(\frac{-\left(E-E_{ct}^{exp}-\lambda^{exp}\right)^2}{4\lambda^{exp}k_BT}\right) \qquad (15)$$

where E_{ct} is the state's energy, the reorganisation energy associated with the transition, and the peak oscillator strength. The superscript "*exp*" denotes that these experimentally fitted values do not account for the CT state energetic disorderσ_{ct}. This is because and are not distinguished by fits of temperature-independent measurements, which gives and .[60]

The CT energy can be expressed as:

(16)

where

$$E_B^{ct} = \frac{-q^2}{4\pi\epsilon_0\epsilon_r r_{ct}} \quad (17)$$

is the binding energy of the CT state and r_{ct} its radius. We stress that in equation (16), IP_D, EA_A and ϵ_r correspond to the energy levels and relative permittivity at the *interface*.

CT states do not, at first sight, lower the Coulomb dissociation barrier and their binding energies remain in the 100-500meV range.[61] Yet, charges are generated efficiently in OPV systems and, from early on,[62] there has been a considerable amount of theoretical work, and more recently experimental work, to explain how CT states dissociate and what provides the driving force ($h\nu > E_g$) for this process. Among the conclusions are that molecular orientations, local environment and disorder significantly impact E_{ct}.[63] Crucially, the overall exciton to charge carrier generation efficiency also strongly depends on the driving force for charge transfer (CT state formation) from excitons, $\Delta G_{CT} = E_{g,opt} - E_{ct}$.

2.3 Morphology

The impact of morphology on virtually all optoelectronic properties of organic semiconductors cannot be understated for both pristine and blend films. We have already alluded to its role in transport, bandwidth, disorder, absorption and charge generation. Controlling the morphology is of direct interest to eliminating the absorption-*FF* trade-off. However, there are two significant issues. The first is that the morphology is hard to control. The second is that it is hard to determine the relevant blend morphology. This is because of a significant range in length-scales, of 'buried' interfaces far from the surface, and of low contrasts stemming from the high carbon content of both the donor and acceptor. Thus it is still not fully clear which aspects of the morphology are most important.

Techniques to study morphology are relatively specialised and their discussion is beyond the scope of this paper. There are however a number of high-quality reviews.[64–68] Ways to

influence morphology usually aim to either orient a molecular axis or to tune domain size and composition. The most common methods include simple thermal annealing,[69] solvent-vapour annealing, which is especially common for solution processed-small molecules,[70] solvent engineering (solvent additives),[71,72] use of templating layers,[73] deposition from hot solution,[40] and synthetic control, especially through side-chains.[74,75] Molecular orientation typically affects transport and extinction coefficient, while domain size and composition correlate to recombination and exciton quenching. There are also less common approaches to tuning the morphology, many of which are covered in ref. [76], a notable one being the use of optoelectronically passive additives.[77] We note that solvent-based techniques offer a degree of freedom, which is not available to vacuum processed OPVs.

2.3.1 Length-scales

A significant issue is that it is still not fully clear what an ideal morphology should look like at various length scales of the BHJ, and whether there is a unique good morphology. Vertical segregation,[78–80] (either obtained from different solubilities and interactions with substrates,[79] or by changing the relative deposition rates during vacuum deposition[80]), domain purity,[81] connectivity,[64,82] and cluster size have all been argued to be important. Furthermore, it is now clear that in binary polymer:fullerene and small molecule:C_{60} blends, a mixed phase (can) co-exist with the pure D an A domains.[66,83,84] This co-existence leads to an energy cascade, which has been suggested to be beneficial in a significant number of works, for example refs. [34,85].

The D-A interfacial morphology should be added to these factors and will be introduced in the context of charge generation. It is therefore, overall, surprisingly difficult to precisely suggest, which of these is most significant and whether any importance ranking is universal. While an in-depth discussion is not possible here, an important message is that the influence of morphology can and often does obscure the influence of the parameters under study.

2.3.4 Side-chains

Typically, non-conjugated side-chains are needed to solubilise polymers, and often small molecules, for both synthesis and device fabrication. It has become clear that these are far from inert and play in fact a significant role in morphology.[65] Their engineering can lead to extremely impressive performances.[40] A particularly striking example of their effect in BHJs is the intercalation of $PC_{61}BM$ in a polymer with long side-chains.[86] Perhaps even more telling is the dramatic influence on performance obtained when changing even short methyl side-chain positions along the backbone in evaporated small molecules, with different optimal depositions for PHJs and BHJs.[74] Lastly, we shall see that docking at the D-A interface is also affected by side-chains.[75]

3. Charge generation and recombination via CT states

3.1 Significance and overview of the processes

In many OPV systems, *IQE*s approach unity. Yet, this efficient charge generation has required sacrificing considerable energy,[61] and there is much room for improvement. This energy loss has manifested in a charge generation-V_{oc} (or loosely an IQE-V_{oc}) trade-off.[1,87] Either the electrical/effective gap is lower than the optical gap, inducing a direct energy loss, or not all excitons are split, inducing a direct current loss. This makes it important to understand the charge generation mechanism and its implications for the recombination pathways.

Figure 5 summarises the relevant processes in charge generation and recombination. Absorption occurs to a singlet excited state of the electron donor or acceptor and is followed by electronic relaxation (thermalisation via internal conversion IC) and geometrical relaxation to the excited-state nuclear configuration. The photo-generated exciton dissociates by electron transfer (ET) or hole transfer (HT) at the donor-acceptor interface, populating the (potentially hot) CT state, which needs to dissociate to free charges. We will refer to the dissociation of

the CT state as 'charge separation' with driving force ΔG_{CS} (in contrast to exciton dissociation by 'charge transfer' with driving force ΔG_{CT}). There have traditionally been two opposing views to explain efficient charge generation despite the prohibitive binding energy. The first is that the CT state is a Coulomb trap, which requires excess energy (hot states) for dissociation to occur. This view has generally been advanced by ultrafast spectroscopy measurements on BHJs,[56,88–93] although some recent experiments have reached the opposite conclusion.[34,94–96] The second view is that dissociation proceeds via a relaxed CT state, which has chiefly been supported by steady-state spectroscopy, charge collection measurements and time-resolved microwave conductivity.[55,58,97,98] The immediate implication is that a CT state has a chance to re-dissociate, as first described by Onsager-Braun theory.[99] **Figure 5**, first suggested by Brédas and Durrant,[24,61] illustrates these two contrasting views.

Experimental data clearly shows that processes involving hot singlet excited states and hot CT states take place. The views diverge in whether these processes are necessary for efficient dissociation to free charges: That is whether the rate of relaxed CT dissociation to free charges k_{diss} is significant compared to the CT recombination rate k_{ct}, or whether hot states are needed to obtain any free charges at all. Recombination is referred to as 'geminate' if the recombining species originate from the same photon. Although the CT state can in principle separate, we will take geminate recombination to mean that this process is inefficient and that the CT state recombines without first dissociating. Geminate recombination is associated with a field-dependent dissociation (and *JV* curve),[85] and is significant for low-performing devices, which has been interpreted as extra energy being needed for dissociation of CT states that otherwise recombine geminately. It is avoided entirely in state-of-the-art systems. Direct recombination from free charges (k_{dir}) can occur via exciton-polaron quenching,[100] traps or, presumably, requires tunnelling of a carrier across the junction to form an S_1 or T_1 exciton.

A crucial intermediate step in bimolecular recombination is the reformation of a CT state from free charges (k_{form}). This process has been described by *Langevin theory*,[60,101] which considers that CT state formation is encounter-limited. In the literature on OPV, *Langevin* '*recombination*' designates a process in which CT state formation is final (no re-dissociation), and therefore describes the rate of bimolecular recombination from free-charges to the ground state as encounter-limited. Despite the original *Langevin theory* simply describing the encounter of ions and not commenting on the fate of the subsequent CT state, we will also take *Langevin 'recombination'* to be final to avoid confusion with the literature. CT state reformation in principle obeys spin statistics, which means 3/4 of events lead to triplet states, enabling T_1 formation as a loss pathway.[102] It is important to stress that the *Langevin* model does not provide an accurate description of OPV systems and entirely fails to predict the V_{oc}.[60,103] The implications of this failure and its remedy by more modern *non-Langevin recombination* theories constitute a key focus of this report. Whether CT states re-dissociate is the key question of this section, which examines microscopic answers. As we shall see in section 4, the macroscopic device properties are difficult to explain in the absence of re-dissociation.

3.2 'Hot CT' dissociation and delocalisation

In optimized OPV systems, the exciton dissociation by ET or HT is generally highly efficient. It is kinetically limited by the rate of exciton diffusion to the D-A interface and by the intrinsic rate of the charge transfer process. The latter is typically ultrafast (at least in polymer:fullerene systems, see below). The former makes the process highly sensitive to morphology. In pBTTT:PCBM systems, it has for example been shown that excitons generated at the interface in intimately mixed donor-acceptor regions lead to ultrafast dissociation, while excitons generated in neat polymer or fullerene regions lead to delayed dissociation, as they first need to reach an interface.[33,34] If an interface is nearby, exciton

diffusion does not need to occur and the ultrafast charge transfer process can compete with electronic relaxation in the presence of excess excitation energy ('hot exciton dissociation'), or can take place from geometrically non-relaxed states.

Pre-thermalisation timescales are usually only accessible by ultrafast spectroscopy. The prototypical measurement is 'transient absorption' spectroscopy (TAS), which optically probes the excited state populations remaining some short delay after an ultra-short 'pump' optical pulse. There is significant evidence that, on short time scales before relaxation occurs, exciton and charge transport in organic semiconductors is ballistic (band-like),[104–109] consistent with lattice or electronic relaxation of the medium and dynamic disorder suppressing the bandwidths (see section 2.2.1). Similarly, the intrinsic charge transfer rate by ET or HT is typically an ultra-fast (20-300 fs) process,[23,110] with timescales depending on the driving force (ΔG_{CT}, free energy difference between the S_1 and CT states) and electronic coupling between the donor and acceptor.[111] Conventional TAS,[56] as well as vibrational spectroscopy,[93] and considerably more sophisticated techniques,[91] show that a quasi-adiabatic separation process can occur on fs timescales and relaxation be by-passed. This means that in the proximity of an interface, excitons can ballistically and coherently reach an interface and yield free charges without relaxing into a low-energy CT state, potentially even entirely bypassing CT states.[56,91] That this process exists is, for example, convincingly demonstrated by the transfer of vibrational coherence from the donor exciton to the donor hole or to acceptor states.[112,113]

The importance of excess energy in the singlet exciton state has been advanced on the basis of kinetics.[33,114,115] However, a TAS study has found no difference with pump energy,[95] somewhat slower pump-charge collection (Time Delayed Collection Field, TDCF) experiments show little or no difference in field-dependence when excess excitation energy is provided,[55,116] and the photocurrent yield in OPV devices is generally independent of excitation energy.[58,117] Thus, exciton dissociation is just as efficient if relaxed electronic

states are excited near the optical 'band-edge', although charge transfer competing with geometric relaxation might still play an important role.

Independently of excess excitation energy and hot singlet exciton dissociation, hot CT states are populated due to the driving force of the charge transfer process (**Figure 5**), i.e. because the S_1 state typically lies above the CT state. The role played by those hot CT states was evidenced from elegant experiments which employ an additional infrared 'push' pulse.[90] This push promotes relaxed CT states to excited ones some time before current collection or probe beam arrival.[90,111,118] The push pulse, which is at extremely early timescales and can therefore not help with charge collection η_{CC}, can increase collected charge by anywhere from -0.5% to +30%.[90] Many of these experiments have been interpreted as hot states yielding more delocalised and therefore less bound *e-h* pairs.[91]

Alternatively, the availability of ionised energy states overlapping with excitonic ones has been suggested to be the key ingredient for charge separation.[118] In this picture, delocalisation of the acceptor increases the number of such states due to narrow band formation. This has been put forward to explain the higher efficiency of donor:fullerene blends having a morphology containing neat fullerene clusters (although an alternative effect on the energetic landscape is discussed in section 3.5). Excess energy in the CT state similarly gives access to more donor energy states, some of which overlap with an accepting state resulting in charge separation.[111,118] Hot CT dissociation has directly been observed by monitoring the absorption change induced by the *e-h* electric field (Stark effect, electro-absorption), which can be used to calculate the distance between charges.[105] The authors concluded that the extremely fast increase in separation was due to coherent motion through fullerene clusters, with a dephasing (localisation) induced by polaron formation (lattice relaxation). Recently, the same group found efficient separation from relaxed CT states for pentacene/C_{60} bilayers, which they explained by a multiple-trapping model, where coherent motion is activated.[96] This hints towards the possibility of re-dissociation of relaxed CT

states on even fast scales. We note that for the recent non-fullerene acceptor BHJs with low driving forces (section 6.2), the charge transfer process might not be ultrafast.[119] However, because the CT state is no longer the lowest energy state, it remains unclear how comparable these systems are to the fullerene-based blends.

3.3 The nano-scale interface

The nano-scale energetic landscape at the D-A interface has been put forward to contribute to the driving force for CT state dissociation, ΔG_{CS}, in spite of the strong binding energy. It has been demonstrated theoretically that the nano-scale molecular arrangement of (small molecule) donors and acceptors considerably affects the energetics.[63] For example, the arrangement of quadrupoles for pentacene molecules sitting face-on relative to C_{60} has been calculated to decrease the energetic charge separation barrier by 400 meV compared to the edge-on configuration, despite a smaller *e-h* distance.[120] Induced dipoles and their directional distribution also lead to non-equivalent site energies along an interface resulting in disorder, which may help with charge dissociation.[121,122] Simulations have similarly highlighted that the interface is not static, which may help dissociation.[123] An interesting finding is that the dielectric mismatch and poor packing at a planar interface leads to an energy alignment favourable to dissociation.[124]

Experimentally, molecular orientation has also been demonstrated a number of times to affect planar interface energy levels. Orientation at model thiophene organic-organic interfaces was directly shown to impact the energetics by ultraviolet photoelectron spectroscopy (UPS).[125] Less directly, templating layers resulting in altered orientations were found to dramatically increase PHJ solar cell performance in ways that could not be explained by absorption or transport.[126,127] Recently, co-existence of different CT states has been found.[128,129] For pentacene/C_{60}, this was assigned to the co-existence of several crystalline phases.[129] Cleaner results were obtained from controlled annealing of rubrene, which results in distinct phases

with highly different CT energies.[130] In BHJs, the influence of the environment has also been investigated by UPS, using a wide range of donor concentrations diluted in C_{60},[131,132] or via measuring CT state energies.[59] The ionization potential (IP) change depends heavily on the donor choice, and ranges from insignificant for amorphous materials up to 600 meV for α-sexithiophene (α-6T). The CT energy of P3HT:$PC_{61}BM$ has been found to differ by a similar amount between the regio-random and regio-regular polymer.[133]

Unfortunately, the morphology at BHJ interfaces is extremely challenging to access. The degree of interfacial orientation, determined by resonant soft X-ray scattering, has however been found to correlate extremely well to J_{sc} and *FF* for a family of polymers with or without fluorine substitution.[134] In another noteworthy study, Graham *et al.* analysed literature data for a significant number of push-pull polymers with varying side chains, and also designed their own set of materials.[75] They found that when steric hindrance favoured fullerene placement on the pull side of the donor, performance was greatly improved. Furthermore, the CT energy width decreased, confirming better conformational selectivity, and the results were backed up by 2D nuclear magnetic resonance. That optimal performance was found with the smallest CT sub-gap absorption tail, suggests that interfacial disorder may not be as critical to charge separation as has been suggested by some theoretical studies. This is backed up by a recent study on a low-disorder polymer:fullerene blend.[135]

3.4 Entropy

When considering the energetics of charge separation in OPV systems, there is an entropy increase associated with CT state dissociation that must be accounted for, and which can also favourably impact ΔG_{CS}.[61,136] This increase stems from the growing number of sites that can be occupied as electrons and holes move away from the interface, lowering the free energy and the Coulomb separation barrier of the CT state. This has recently become an important consideration in charge generation.[61,88] Assuming a fixed hole, Gregg found that, since the

number of sites scales as the available surface, dimensionality dramatically affects the entropy increase.[137] While there is no gain for a 1-D chain, entropy reduces the charge separation barrier from 270 meV to 5 meV for a 3-D model.[137] It was therefore suggested that fullerenes might be successful precisely because of their 3-D electronic coupling.

Conceptually, the fixed hole treatment corresponds better to de-trapping of an electron than charge separation at a D-A interface. Given the influence of dimensionality, the author suggested that the barrier decrease caused by entropy would become less significant going to a PHJ and even less significant for a BHJ.

In a significant recent contribution, Hood and Kassal studied the full PHJ problem with the hole allowed to move.[138] For *localised* carriers on a model hexagonal close-packed lattice with nearest neighbours at 1nm and ϵ_r 3.5 at the PHJ, they found that the space that holes can occupy decreases the escape distance from about 8nm for fixed holes to 5nm for mobile holes. In this picture, it is the restriction of carriers to segregated D and A phases that is beneficial. Furthermore, the interplay of disorder and entropy was considered. In disordered media, the entropic contribution is decreased because low-lying energy sites are preferentially occupied, reducing the number of conformations. This however is offset by the disorder's contribution (reduction in Coulomb barrier), which overall facilitates separation. The authors noted however that, while the average randomly generated disordered energy landscape helps separation, some generated landscapes lead to deep traps and hinder separation. This effect is most pronounced for highly disordered landscaped. Interestingly, the (significant) degeneracy of CT states, which diminishes the entropic gain, has not been discussed much with respect to entropy.[60,139]

Entropy describes the energetics and not kinetics of charge separation and its role in charge dissociation is consequently debated.[118,138] The temperature-independence of generation reported in some studies has thus been taken as an indication that separation is attempt-limited rather than thermodynamically limited, which would discredit entropy.[118] This problem was

also found in early Monte-Carlo (MC) simulations. These often required unrealistic CT state lifetimes (number of attempts) to achieve efficient dissociation at low-field, including in the presence of disorder (see ref. [85] for a summary of values). This problem can be mitigated by including delocalisation along the polymer chain,[140] or experimentally observed high local mobilities,[85] which are both linked to entropy. If, moreover, the energetic landscape induced by the co-existence of neat and intermixed D-A phases is taken into account, the high experimental OPV yields at even low fields are recovered.[85,141] Thus, polymer systems likely benefit from intrachain coherent motion (leading to high local mobility) while all-small-molecule systems may be helped by the presence of (fullerene) aggregates. Whether efficient all-small-molecule non-fullerene blends can be realised consequently remains to be seen.

Experimental evidence for the role of entropy is also growing. Time-resolved electric-field induced second harmonic generation (TREFISH) measurements combined with analytic calculations and MC modelling have found early time diffusion to explain efficient, field-independent separation in P3HT:PCBM.[142] The experiments monitor the *e-h* field, much like electroabsorption, but the field is probed by the change in intensity it induces in the second harmonic signal caused by the probe pulses. More recently, the vacuum-semiconductor interface has been used as a model system.[143] Here, the semiconductor is ionised by a UV photon and the resulting charge forms a CT-like complex with its image charge. After a variable delay, the CT-like complex is ionised and the photo-electron analysed as in a standard UPS experiment (time-resolved two-photon photoemission). This showed an extremely rapid energetically uphill motion of the CT-like state.

4. Thermodynamics of CT states

Having discussed charge generation and important microscopic concepts specific to the OPV field, we now consider their implications for the thermodynamics of a full device. The key theme is that experimental V_{oc} data can currently only be explained if CT states have a

significant re-dissociation probability ($k_{diss}>>k_{form}$). This cannot easily be reconciled with CT dissociation occurring exclusively via hot states. There have been several good discussions about the decrease in the SQ efficiency limit resulting from the presence of a sub-gap Gaussian CT absorption tail and a driving force requirement.[26,52,54,144–146] These semi-empirical modifications to detailed-balance were mostly motivated by the important observation that the V_{oc} scales not with the optical gap but with CT state energy, with a loss of about 600meV with respect to E_{ct} for virtually all studied systems.[52] In this section, we will focus on the recent landmark account by Burke *et al.*,[60] since it is the first to derive the V_{oc} entirely from fundamental principles and provides important insights. We note however, that the works of Kirchartz and Tress are also noteworthy in this respect.[103,147]

4.1 Non-Langevin recombination

According to the Jablonski diagram in **figure 5** and the discussion in section 3.1, in the absence of CT state re-dissociation ($k_{diss}<<k_{form}$) and ignoring k_{dir}, the bimolecular recombination rate is simply the rate of CT state formation k_{form}, which is described by Langevin *theory.*[101] This theory considers that exciton (or in the case of OPV CT state) re-formation is limited by the ability of charged species to find each other, such that:

$k_{lan} = k_{form} = \beta_{lan} npdV$ with E_g (18)

with dV as a volume element, and $h\nu > E_g$ and V_{oc}^{SQ} being the electron and hole mobility. Langevin *recombination* predicts that bimolecular recombination corresponds to CT re-formation $k_{bimol} = k_{lan}$ (no CT re-dissociation) and effectively predicts charge recombination in OLEDs, as they are optimized for efficient (radiative) charge recombination.[60] It however considerably overestimates the recombination rates found in OPV systems.[148,149] There have been several attempts to modify the Langevin prefactor [148], including considering only

the slower carrier,[150] and accounting for the geometrical constraints imposed by BHJ donor and acceptor phases.[151,152] The experimental temperature-dependence of the pre-factor can however only be recovered considering the spatial charge distribution,[153] or by allowing for CT state re-dissociation (Onsager-Braun theory).[98,154] An important side note is that considering the spatial distribution of charges is essential for a proper evaluation of recombination from charge extraction measurements. Ignoring it typically leads to artificial recombination orders (see refs [153,155,156] for details). In short, in a device of thickness *d*, the electrons and holes are typically not homogeneously distributed, such that:

$$\Delta V_{oc}^{SQ} = E_g / q - V_{oc}^{SQ} \qquad (19)$$

where and E_g are the recombination rates obtained with the inhomogeneous and homogeneous distribution, respectively. Since , a typical analysis in terms of k_{nr} fails.

Regardless of spatial effects, Langevin recombination predicts a decrease in *FF* with mobility,[103] which is not necessarily experimentally observed.[157] Above all, Langevin recombination predicts $V_{oc}(T)$ incorrectly as:[60,103]

(20)

This reproduces neither the qV_{oc} - E_{ct} trend nor the temperature dependence of V_{oc}, which approaches $\hbar\omega_m$ and not at low temperatures. This discrepancy can however be solved by allowing CT states to re-dissociate.[60,103] Langevin recombination would then be applicable mostly to OLEDs, because these are optimised to avoid re-dissociation of charges (efficient exciton recombination is sought), and not to OPV systems, because these are optimised for charge separation to occur.[60] Note that in this picture, low-performance OPV systems with high geminate recombination are poor precisely because they more resemble OLEDs. For

clarity, we highlight again that hot CT state dissociation *necessarily* implies (modified) Langevin recombination since it considers the CT state to be a trap (or alternatively the primary recombination channel is not via the CT state). However, given the wealth of data on CT luminescence and its correlation to V_{oc}, this seems unreasonable.

4.2 Equilibrium

The derivation of the V_{oc} in OPV systems by Burke *et al.* follows an elegant chemical-potential approach identical to the one we introduced in section 2.[60] In other words, before recombination via a CT state, a charge pair will dissociate and reform several times. This is not easy to prove, but is made plausible by high local and short time mobilities, as well as by delocalisation, which allow charges to sample the energetic landscape (e.g. many hops) before they recombine (c.f. section 3.4).[85,94,142,158] In an equilibrium picture, by detailed balance and assuming Langevin CT state formation, the dissociation probability must also depend on the relative concentrations of CT state and free charges, as well as on their mobility.[144] When CT state re-dissociation is possible, the reduction factor γ in the recombination rate compared to Langevin theory:

$$\gamma = \frac{k_{ct}}{k_{ct}+k_{diss}} \qquad (21)$$

becomes a metric of equilibrium, with low values corresponding to numerous re-dissociation events (exchanges between CT states and free charges)[60,103]. The experimental reduction factors in the 10^{-1}-10^{-3} range are consistent with an equilibrium description but do not invalidate other theories.[140] Equilibrium-picture drift-diffusion simulations have successfully reproduced V_{oc} of pentacene/C_{60} bilayers with realistic CT lifetimes of 1-10 ns.[159] Finally an interesting point is that CT absorption and emission spectra are related by detailed balance,[52,54] which implies they are in equilibrium with the environment. Provided charges are also in equilibrium, this is in our opinion further evidence for the rapid exchange. It is

important to note that equilibrium makes $E_j/\hbar\omega_m$ harder to measure, since it implies that effective rate constants are measured by decay experiments.[60]

4.3 V_{oc} of an organic solar cell

Assuming equilibrium, the *e-h* pair recombination rate is given by:

(22)

and the CT state population density n_{ct} can be described by chemical potentials as was done for electrons and holes in section 2.1. Then, assuming Boltzmann statistics and a Gaussian density of CT states (DOS) $\hbar\omega_m$ with width σ_{ct}, the CT state density can be calculated and the V_{oc} deduced from equations (22) and (11):[4,60]

$$qV_{oc} = E_{CT} - \frac{\sigma_{ct}^2}{2k_BT} - k_BTln \qquad (23)$$

where $f_{int}N_0$ is the effective density of CT states, which is the effective density of charge carrier states scaled by f_{int}, the volume fraction of the solar cell that is interfacial.

The losses compared to the optical gap can be separated into three terms: a driving force loss , a non-radiative loss , and a 'radiative' loss $q\Delta V_{rad}$. Since some radiative losses cannot be avoided (section 2.1), it is more instructive to consider the additional loss compared to the ideal case $\Delta V_{rad}^{OPV} = \Delta V_{rad} - \Delta V_{oc}^{SQ}$. This is due to disorder and short CT lifetimes and would still exist without a driving force and if all recombination was radiative.[54,60]

We stress that the arguments above are identical whether recombination via CT states is radiative or not. Equation (23) implies that even with fully radiative recombination, a V_{oc} loss is incurred from disorder due to the presence of the subgap CT states ( ). Considering the low CT state luminescence, an additional and severe penalty must be added.[4,54] For low

EQE_{EL},  , so that both logarithmic terms in equation (23) are related. While this expression is not entirely new (disorder and CT state dark current have been considered previously),[54,103,146] it is both complete and unambiguous. Above all, it is derived from fundamental principles and rests on clear assumptions. These are that equilibrium between CT states and free charges exists, and that at V_{oc} all recombination occurs via a CT state. We note that OPV systems with a single neat material (no complementary D and A) have low currents but a high V_{oc}, which must originate from excitons, since charges are inefficiently generated. Thus, in retrospect it is not surprising that CT excitons should determine the V_{oc}.

4.4 Opportunities to improve V_{oc}

From equation (23), different opportunities to improve the V_{oc} can be assessed.[60] The biggest gain can be expected from reducing the driving force $FC=\left|\chi_{GS}\vee\chi_{exc}\right|^2$ and from reducing the interfacial energetic disorder σ_{ct}. Experimentally, a detailed study on a polymer:$PC_{61}BM$ blend has attributed the high obtained V_{oc} to low disorder,[135] and NFAs achieve high EQEs at low ΔV_{driv} (see section 6). Because high EQEs were previously not believed to be achievable at low driving forces, increasing  (decreasing the CT state binding energy) was considered.[60,160] For polymer:fullerene blends, the relative permittivity has been found to correlate well with the V_{oc} loss,[161] and its increase has sometimes resulted in enhanced performance,[162,163] though efficiencies remained very low.[a]

By contrast, the other terms in equation (23) vary only logarithmically and should offer comparably low gains. This low impact has been suggested to explain the relatively constant loss of 0.6V observed for many systems.[60] However, they still represent a significant loss source. The best reported EQE_{EL} for an OPV system is only 10^{-4},[164] which represents a V_{oc}

[a] Note that we deliberately avoid the term dielectric constant since ϵ_r) depends on frequency.

loss of 230mV at a V_{oc} of 1V. It is important to note, that increasing the lifetime of the CT state also improves EQE_{EL} with:

$$EQE_{EL} = \frac{k_{rad}}{k_{rad}+k_{nr}} = \frac{1}{1+\tau_{rad}/\tau_{ct}} \approx \frac{\tau_{ct}}{\tau_{rad}}\ 10^{-4} - 10^{-6} \qquad (24)$$

where $\tau_{nr} \approx \tau_{ct}$ and $qV_{oc} = E_g + k_B T \ln\left(\frac{np}{N_c N_v}\right) + k_B T \ln(EQE_{EL})$ because of the extremely low luminescence yields. Hence, we expect that a thousand-fold improvement in τ_{ct} yields twice the ΔV_{oc} =120 mV reduction estimated by Burke *et al*. Given that PL quenching of the S_1 state has been a widely used metric to evidence successful charge generation, it may be surprising that higher EQE_{EL} and PL yields are desirable for OPV systems as well. To be clear, emission is desirable only if it occurs after charge dissociation (as opposed to from exciton or geminate CT state recombination). That (total) PL quenching has correlated so well to exciton quenching is due to the very low CT state emission efficiency. As we discuss in section 6, where we expand on k_{nr}, this is not fully true for 16-20% efficient OPVs.

An interesting problem is the degeneracy of CT states. To reproduce experimental data, degeneracies in the order of 30 CT states per acceptor molecule for a CT state radius of 2.5nm are needed, which implies long-range CT formation.[60] This would suggest that increasing delocalisation has a negative impact on V_{oc}. In a recent experimental study, which decomposed the CT oscillator strength into coupling strength (estimated from PL lifetime) and number of states, the degeneracy was found to be in the range of 5-60, in agreement with the above estimation.[139] Since delocalisation is understood to play an important role in dissociation, and since ϵ_r, r_{ct} and the CT binding energy should all correlate, this needs further investigation.

4.5 Other recombination mechanisms

So far, we have exclusively discussed recombination via CT states. This is of course not the only pathway. Tail states and traps,[144,155] and triplet states,[102] can also play a significant role.

These however cannot explain V_{oc}, since to our knowledge, its dependence on E_{ct} cannot be recovered. An important point is that the dominant recombination mechanism has been found to change with carrier density from trap-assisted to bimolecular.[165] Thus traps could be more relevant in determining the *FF* than V_{oc}. Our own view is that recombination via CT states is the dominant mechanism at V_{oc} in good devices. Lastly, recombination via triplets poses an interesting challenge, since the S_1 and CT states need identical energies to obtain high V_{oc}, which implies a triplet trap.[102] Whether this is best overcome by a low or a high S-T splitting (T re-dissociation or gap law) is currently not clear in our opinion.

5. The fill factor: charge extraction, traps and morphology

The *FF* is determined by a competition between charge extraction and recombination at different bias voltages,[2,29,166] and typically decreases severely with active layer thickness.[29,167,168] This is a problem, first because a high *FF* is required for efficient devices, and secondly because the decrease with thickness leads to an *FF*-absorption trade-off. Typically, optimal polymer:fullerene performance is obtained around 100 nm active layer thickness, while ~300nm are needed for complete absorption across the spectrum.[29] This problem is even more evident for small-molecule devices, which rarely work well beyond 250nm active layer thickness. In addition, solution processing is not considered scalable for thicknesses inferior to 250nm, because uniformity becomes problematic.

5.1 Mobility, space charge and recombination

The low carrier mobilities of OPV materials mean that there is a significant charge population at operating conditions compared to high quality inorganic devices (ideal Shockley diodes).[169] This excess charge can recombine, reducing the free energy and current. In macroscopic terms, the additional charges create a space charge region free of electric fields, through which carriers must diffuse.[29] Since the concentration gradient is low in the space

charge region, the transport is extremely inefficient. When the entire active layer is occupied by a space charge, the external field V_{ext} is entirely screened by the internal field V_{int} caused by the space charge and the device is effectively at V_{oc}.[b] By calculating the internal field, *JV* curves can be reproduced analytically with great fidelity,[169] a process which normally demands drift-diffusion modelling. An interesting point is that the existence of V_{int} (due to low mobilities) makes the non-ideal diode equation invalid and the determination of ideality factors and series resistance problematic.[169] An accurate method based on illumination intensity (*I*) dependent np curves has however recently been proposed.[170] There seems to be consensus that to achieve a target *FF*=0.7-0.8, mobilities in the 10^{-2} $cm^2V^{-1}s^{-1}$ range are required.[29,103,171] This of course depends on the recombination strength,[29,103,166] and good fits to experimental *FF*s are found by using a single k_{rec}/k_{extr} parameter.[166] The simulation work of Tress is particularly interesting in this respect, because it considers the effect of different recombination mechanisms, including Shockley-Read-Hall (SRH), on *FF*.[103] Others have considered only Langevin or constant bimolecular recombination. In all cases, except for Langevin recombination, high mobilities are beneficial. SRH recombination was found to limit *FF* to 0.7, marginally better than for Langevin, but this may depend on simulation parameters. For P3HT:$PC_{61}BM$ and (reduced) bimolecular recombination, it was calculated that with current mobilities, the recombination rate must be reduced a hundred times to reach the *FF* target.[29] As a single parameter and from a study of numerous systems, k_{rec}/k_{extr} 10^{-4} is needed.[166] Note that none of these studies consider dispersive transport.

Another interesting point is whether both charge carrier mobilities need to be balanced. One study on solution-processed small molecule fullerene blends found that balanced mobilities were necessary.[171] By contrast, *FF*=0.66 can be achieved at 8% donor (by volume) diluted in C_{70},[172] a system with extremely imbalanced (but low) mobilities. These different

[b] i.e. the device is a charged capacitor.

observations are likely explained by different recombination mechanisms. For Langevin recombination, balanced mobilities are desirable.[103] However, this becomes irrelevant if CT dissociation is possible and equilibrium holds since, by detailed balance, the recombination becomes independent of mobility.[103] Given the above discussion, a short answer should be that the lower mobility limits *FF*.

6. New systems

New small molecule systems are challenging our conventional understanding of OPVs. 'Dilute HJ' devices (**figure 4e**) seem to invalidate the traditional morphology paradigm of percolating separated D and A phases. NFAs bring into question the need for a driving force for interfacial charge transfer, as well as our previous empirical estimates of the achievable PCEs. This section highlights the key features of these new systems, presents the current understanding of dilute HJs and attempts an initial explanation of the high NFA performance.

6.1 Dilute heterojunctions

Zhang *et al.* found that for many small molecule:C_{60} BHJs, the optimal performance was, surprisingly, obtained at only 5% volume donor.[173] Currents were limited by the low absorption of C_{60}, but *IQE*, *FF* and V_{oc} improved significantly compared to standard BHJs with higher donor content. With the more absorbing fullerene C_{70} , PCEs of 8.1% have been achieved in optimised devices.[172] While it is unlikely that these systems can become commercially relevant, they are important for a number of reasons. First, these so-called "dilute" OPV cells represent an important model system, in which the morphology can be de-correlated from other parameters under study. In particular, different donors can be more directly compared. Second, they provide interesting case studies for the *FF* and for the effect of delocalisation on charge generation. Last, they demonstrate that percolating neat donor phases are not as critical as previously thought. We note that while the dilute concept so far

882works best with (vacuum processed) small molecules and C_{60} or C_{70},[c] it is also applicable to
883solution-processed polymer:fullerene blends,[174] where it has been used as a model system.[75]
884Given the chain-like nature of the polymers though, percolation pathways are more likely at
885the ratios used there.
886
887
8886.1.1 *Morphology*
889Observing the CT absorption at low donor concentrations, Vandewal *et al*. showed that the
890number of CT states scaled linearly with donor concentration for dilute TAPC:C_{60} devices
891(4,4'-cyclohexylidenebis[N,N-bis(4-methylphenyl)benzenamine]:C_{60}).[175] The implication is
892that each donor is in a CT state and thus surrounded by fullerenes, hence our name 'dilute'
893(**figure 4e)**).
894It is important to note that the relative number of CT states was only accessible in that study
895because E_{ct} did not change with TAPC concentration, a point we will elaborate on below.
896That the devices work despite the donor not forming a segregated neat phase but instead being
897surrounded by C_{60} molecules, clearly invalidates early understanding of the desirable
898morphology. It also means that the donor environment in a dilute HJ is, to a good
899approximation, identical for all donors. For another donor, α-6T, the fact that the donor
900molecules at low concentration are surrounded by fullerenes is also convincingly evidenced
901by the sudden shift in E_{ct} and donor IP, which occurs around 30% α-6T concentration in C_{60}
902and is attributed to aggregation (α-6T π-π stacking).[59,131] More generally, it has been
903observed for a number of donors that the C_{60} packing is not significantly disturbed at low
904donor concentrations of up to ~15%, though the fullerene domain size decreases.[132,176,177] For
905C_{70}, crystalline neat fullerene and amorphous mixed donor-fullerene regions have been found

[c] We are not aware of any examples with solution-processed small molecules only.

to co-exist from CT state energies and electron microscopy.[128] To our knowledge, the situation has not been investigated for $PC_{61}BM$.

6.1.2 *Energetics*

The E_{ct} has been studied in dilute systems for a large number of materials.[59] Although there have been fewer donors for which the effect of concentration has been tested at very dilute ratios, no significant changes in E_{ct} were observed when the donor concentration was lowered starting from ~15% for either TAPC or α-6T. [59]

The effect concentration on IP and E_{ct} has been studied more extensively at 10-50% ratios.[131,132] At higher concentrations, E_{ct} remains near constant for TAPC while, as discussed above, a strong shift in CT energy is found for α-6T. The IP shift of C_{60} and donor caused by changes in stoichiometry, is predominately determined by the relative polarisabilities of the blend components (c.f. equation **12**).[131] For rubrene for example, which has a similar polarisability to C_{60}, the IPs are largely unaffected by donor concentration. The opposite is true for α-6T. Since hole and electron polarisabilities are similar, the C_{60} electron affinity (EA) can also be estimated.[131]

Looking at the implications on device performance, E_{ct} has been found to determine the $\underline{V_{oc}}$ of dilute HJs for a wide range of materials,[9] similar to more common donor:acceptor mixing ratios and contrary to some initial reports. The V_{oc} losses are however somewhat decreased compared to standard BHJs due to a reduced number of CT states,[175] in line with predictions by equation (23).

6.1.3 *Delocalisation*

In principle, dilution in these systems provides a good probe for the effects of delocalisation. This is first because the absence of donor delocalisation and the progressive growth of C_{60} cluster size in the dilute region.[132,176,178,179] This provides a nearly continuous variation in

electron delocalisation with relatively small changes in hole delocalisation. While few time-resolved spectroscopic studies have been carried out on the dilute model systems, those would provide an excellent appreciation of the impact of the delocalization on the charge generation.

From studying the CT-induced electro-absorption, Bernardo *et al.* found that the CT states become increasingly polarisable and therefore delocalised with decreasing amount of NPD in C_{60} (*N,N'*-di(1-naphthyl)-*N,N'*-diphenyl-(1,1'-biphenyl)-4,4'-diamine, an amorphous small molecule commonly used in OLEDs).[176] The CT state energy decreases with delocalisation in those devices and could not be entirely explained by the change of dielectric constant with increasing C_{60} content (in general, the change in dielectric constant has not been found to correlate with CT energy).[128,132,176] The greatly enhanced IQE at dilute ratios was attributed to delocalisation, . Similar conclusions were reached with DBP:C_{70} (Dibenzo{[f,f]-4,4,7,7-tetraphenyl}diindeno[1,2,3-cd:1,2,3-lm]perylene:C_{70}),.[128]

6.1.4 *Transport and recombination*

Dilute systems are also an interesting case study for the *FF-absorption* trade-off. From equation (23), the reduced number of CT states in these solar cells slows down recombination and explains the increase in V_{oc}.[55] Somewhat counter-intuitively, the number of CT states is very small and roughly corresponds to the number of CT states in PHJs.[175] The increase in *FF* with dilution down to 5% donor, despite the drastic decrease in μ_h, can be understood as originating from the slowed-down recombination (and improved CT state dissociation via increased C_{60} delocalisation). The delocalisation is also expected to facilitate CT re-dissociation, which could further reduces the effective recombination rate.[103] Computational studies have suggested that delocalisation has two opposite effects on the non-radiative rate. The decreased *e-h* overlap reduces the non-radiative recombination, while the decrease in CT

energy caused by delocalisation (only sometimes observed)[128,132,176] has a negative impact via the gap law.[180]

Thus, overall an *FF*=0.66 can be achieved at 8% volume donor in C_{70},[172] despite very low μ_h. Below 5% donor, the benefit of slower recombination is outweighed by the slowed transport and the device performance decreases.[173] That the holes are transported at such low donor concentrations is at first sight extremely surprising. A spectroscopic study has recently found the mechanism to be long-range tunnelling between the donor sites, which is possible for estimated donor site distances of 4 nm.[181] It is however difficult to entirely exclude the existence of percolating transport pathways at 5% donor concentration.

6.2 Non-fullerene acceptors

The most exciting recent development in the OPV field is the emergence of non-fullerene acceptors (NFAs).[119,164,167,182–186] These have rapidly risen in performance to reach a single-junction certified PCE of 13%, the current OPV record.[187]

NFAs exhibit significant advantages compared to fullerenes. The first is that, when designing new organic molecules, chemists have to balance many factors including cost, device-fabrication, absorption, packing, morphology, transport and energy levels. Fullerenes have a very limited tuneability, meaning that all the optimisation rests on the donor, and making the synthetic challenge formidable. By contrast, the energy levels of NFAs can be tuned (for example by fluorination), their packing influenced (for example with modification of side-chains), and their absorption engineered by varying the core moieties. This also means that the donor and acceptor can be designed together, which is especially attractive, given the importance of the molecular arrangement at the D-A HJ (section 3.3). Secondly, the limited active layer thickness in OPVs, caused by poor charge carrier transport, makes strong absorption imperative. Yet, commercially relevant (C_{60}-based) fullerenes have a poor

absorption match to the solar spectrum, exacerbating the *FF-absorption* trade-off. On the other hand, NFAs show strong absorption in the relevant spectral region, and again the donor and NFA can be designed together to complement each other in absorption. Third, fullerene films suffer from stability issues (i.e. oxidation, photo-polymerisation and morphological ripening).[66,188–190] There is growing evidence that NFAs can resolve some of these. [191,192] Last but most importantly, devices employing NFAs exhibit a reduced charge generation-V_{oc} (*IQE*-V_{oc}) trade-off. Understanding why and to what extent this trade-off is reduced using NFAs is in our opinion currently one of the most pressing scientific questions in the OPV field, and it will require insights from both device physics and spectroscopy.

Given the very recent appearance of NFAs, there are many other aspects that remain to be studied. These range from blend morphology and charge transport, to explaining what makes twisted perylenes and 'ITIC-like' molecules (A-D-A triads with bulky acceptor groups and sterically hindered donor cores) so successful.[193,194] These are beyond the scope of the current report, where we shall focus on the reduced V_{oc} losses and reduced driving force requirements characteristic of high-performance NFAs.

6.2.1 *Reduced charge generation-V_{oc} trade-off*

A first significant V_{oc} loss in OPV systems is due to the driving for of exciton dissociation (), which for fullerene devices typically cannot be reduced under ~100 meV without resulting in very low IQEs.[195] Indeed, while an efficient polymer:fullerene system with a low driving force for ET has been reported,[1] the charge transfer was found to be slow and inefficient. On the other hand, polymer:NFA systems without significant driving force for either the ET process (with polymer excitation) or the HT process (with NFA excitation) show fast and efficient exciton dissociation.[119,196–198] It still needs to be established whether the intrinsic charge transfer (not limited by exciton diffusion) occurs on the 100-*fs* time scale (like in polymer:fullerene blends) or is slightly slower (picosecond regime), but it is clear that

the excitons dissociate. The driving force requirement for charge separation in OPVs has sometimes been analysed graphically as in **figure 6**,[164,199,200] where we show a compilation of literature data (expanded from that reported in previous work). The EQE_{max} (representative of charge generation efficiency) is plotted as a function of $E_{g,opt}$ - qV_{oc}. The grey line corresponds to the least severe trade-off we obtained from 2016 data with NFAs. Recent results from 2017 are strong evidence for an even weaker trade-off (dashed black line).[51,201] There are now several polymer:NFA blends that achieve high *IQE*s at $\Delta V_{driv} \approx 0$ and comparatively low V_{oc} losses (diamonds along dashed line in **figure 6**).[119,164] For comparison, a fit with high performance fullerene devices is included and the record devices for $PC_{61}BM$ and NFAs are indicated with an arrow.

6.2.2 *Quantifying the charge generation-V_{oc} trade-off*

While we cannot suggest a better metric than the one shown in **figure 6** at this point, it is important to realise that this graphical method is far from perfect. First, the generation efficiency is difficult to define since it is voltage dependent. The *FF* can also be affected by the generation-V_{oc} trade-off, which is not captured by an EQE_{max}(V=0)-ΔV_{oc} graph. Second, at V=0, the generation efficiency corresponds to the *IQE.* This quantity is, however, not usually reported and the EQE_{max} must be used in assessing the generation-V_{oc} trade-off. It is then tacitly assumed that the EQE_{max} is not limited by absorption. Xu *et al.* have recently reported near 100% IQE at the optical onset with a very low $\Delta V_{oc} = 0.49V$ (**figure 6**, top left diamond).[201] This strongly suggests that the EQE_{max}-ΔV_{oc} graph *overestimates* the trade-off. Third, the optical gap is somewhat hard to accurately define for an OPV device since there is typically a long absorption tail: $E_{g,opt}$ values must always be treated with caution. A sensible definition is the point at which the tangent at the absorption inflexion crosses the origin. Last, $E_{g,opt}$ incorporates additional terms not directly related to the driving force. An additional

challenge to asses only the driving force, is that at small values, must be measured by comparing the EL spectrum of the blend and neat films, which is accessible to few groups, and changes in aggregation should also be accounted for. Altogether, it may no longer be desirable to compare fullerene and NFAs on the same graph. Perhaps a more appropriate comparison should now be the influence of driving force on *FF*, adjusted for charge carrier transport using for example the methodology of Würfel *et al.*[169]

6.2.3 *Increased electroluminescence yield*

Since the champion fullerene device exhibits a $E_{g,elec}$ and the second best reported NFA device a , the avoided $E_{g,elec}=IP-EA=$¿ of ~100meV far from fully explains the improvement.[40,201] A second and equally significant source of improvement for high-performance NFAs is their comparatively high EQE_{EL} (see equation 23), which reduces . There is an important difference between systems with small and large ΔV_{driv}: For a series of polymer:NFA blends, Liu *et al.* have found that the EQE_{EL} increases by two orders of magnitude to $5x10^{-5}$, when $q\Delta V_{driv}$is reduced from 370 meV to ≈0.[119] Baran *et al.* have also reported record EQE_{EL} of IP at negligible EA .[164] This indicates that the alignment of the S_1 and CT states also plays a role in enhancing the EQE_{EL}. Most interestingly, for these low driving forces, the emission of the blend and neat material could not be distinguished in either work. In other words, the emission is no longer predominantly from CT states but from the singlet excited state of the blend material with the lowest energy gap or of an S_1-CT hybrid state. Such mixing is known to occur when the states are close in energy, e.g. in C_{60}.[202] This effect does not appear to be unique to NFAs though: Kawashima *et al.* have observed, from PL, the same effect with $PC_{61}BM$.[1]

At the low emission yields found in OPVs, the EQE_{EL} corresponds to ~ as shown by equation (24). The expressions for these are obtained from Fermi's Golden rule and are formally similar:

$$k_{rad} = \sum_{j_{vib}} k_{rad,j} = \frac{2\pi}{\hbar}\rho\left|\mu_{opt}\right|^2 \sum_{j_{vib}} FC_{rad,j} \qquad (25a)$$

$$k_{nr} = \frac{2\pi}{\hbar}\rho\left|U_Q\right|^2 FC_{nr} \qquad (25b)$$

where *FC* is the Franck-Condon factor, is the DOS of final states, and is the rate associated with the emission from the *0*th vibrational mode of the excited state to the *j*th vibrational mode of the ground state (a single line in the Franck-Condon progression). E_g^{DA} is the transition dipole moment, and U_Q is the electronic coupling terms between the electronic states. In the simplest case, which is a displaced oscillator (identical nuclear potential curvatures for the excited state and GS as in **figure 2**), the total emission rate is:

$$k_{rad} = \frac{2\pi}{\hbar}\rho\left|\mu_{opt}\right|^2 \qquad (26)$$

Crucially, given that the oscillator strength is considerably smaller for CT emission than for S_1 emission,[203] the EQE_{EL} increase observed for higher performance NFAs cannot directly be interpreted as a reduction in the non-radiative recombination rate. As was mentioned above, we expect that a significant part of the EQE_{EL} gain is simply because emission no longer proceeds from a CT state but from either a S_1 or a hybrid S_1-CT state with higher oscillator strength. For clarity, when comparing emission from CT states, the relative EQE_{EL} can safely be interpreted as a change in $E_g^{DA}-E_{g,opt}$, as long as there is no significant change in the CT-S_1 mixing. This is because both k_{rad} and k_{nr} approximately scale with the change in dipole moment between the GS and CT state.[9,204]

6.2.4 *Non-radiative recombination*

While a higher oscillator strength can potentially explain most of the improved emission yield in NFA systems, the decrease in charge generation-V_{oc} trade-off also suggests a slowed down from the CT state (or S_1 or hybrid S_1-CT state) and an increased available time for charge separation (i.e. number of possible charge separation attempts). Decreasing also offers twice greater V_{oc} gain than increasing ϵ_0, ϵ_r, since according to equation (23), it also reduces . In principle, a smaller can also diminish the requirements on charge extraction and improve the *FF*. There are too few spectroscopic studies at the moment to conclusively comment about the fraction of increased EQE_{EL} originating from a decreased . Nonetheless, some comparisons can be made. Following our earlier discussion, there are two conceivable sources for a reduced : A favourable D-A molecular docking decreasing the coupling U_Q between the CT state and GS, and a reduced Franck-Condon factor.

Only detailed computational and careful experimental studies can determine U_Q. Though these are time-consuming and thus cannot be applied to a large number of D:A combinations, they may help in the future to identify the desirable molecular motifs. By contrast, it is possible to make preliminary observations on the *FC* term, for which Benduhm *et al.* have recently stressed the role of *intra*-molecular vibrational modes.[9] Here, contributions from high-frequency vibrations dominate, although for CT states, a contribution from the slow reorganisation of the environment is also present (low-frequency intra-molecular modes).[9,59] The reorganisation energy associated with these low-energy vibrations effectively reduces the energy gap from E_{ct} to :[9,204–206]

(27)

thus increasing η_{ec} (equation (25b)). Here, η_{Diss} is the dominant vibrational frequency in the non-radiative transition, is the average vibration frequency of the molecule, and η_{cc} is the

reorganisation energy associated with intra-molecular rearrangements. Much like [ ] we expect disorder to cause an effective reduction of the gap and to increase η_{ec}. Since the emitting state of NFAs remains unclear, it is worth pointing out that, for intra-molecular vibrations, the expression for [ ] is analogous with η_{cc}.[207] Depending on the character of the emissive state in NFAs, this could represent a first reduction in [ ]. A low α_{ct} should also increase the gap and reduce [ ].

Though the effective vibration energy of 160meV (linked to C-C benzene breathing mode) found in fullerene-based systems has been argued to be fundamental, it is worth assessing whether NFAs offer an opportunity to decrease it. To this end, we simply estimate E_{ct} from the (photo- or electroluminescence) emission spectra of NFA blends exhibiting vibronic progressions (the fits are shown in the S.I., we refer the reader to ref. [208] for a summary of emission features in solids and why absorption cannot be used). The results obtained from fits of literature data are summarised in **table 1** (note that our results do not stem from dedicated measurements and are therefore likely to be approximate. Similarly it is likely that PCBM has a much higher vibration energy than C_{60}, which is in line with recent computational results.[209]). For CT emission, the vibronic progression is usually not accessible due to the high re-organization energy and disorder but for recent NFA systems with low V_{oc} losses, the vibronic spacing is resolved and as small as ~130 meV. This is considerably smaller than the value found for fullerene systems and, given the super-exponential dependence of [ ] on λ (equation 27), represents a 20-500 fold decrease in non-radiative recombination rate compared to rubrene:C_{60}. As illustrated in **table S2**, the value depends considerably on the other calculation parameters, but can clearly account for a significant fraction or all of the 100-fold EQE_{EL} increase found for NFAs. From a very simple estimate, using reported EQE_{EL} values, [ ] meV is required to reach the ~1% EQE_{EL} values achieved by perovskite devices, although lower vibrational energies are also expected to increase the influence of

traps.[7] It is important to note that for many high performance NFAs (but not usually for ITIC), emission occurs from the polymer. For hybrid S_1-CT states we would expect that the vibrational mode energy of the blend material with the lowest gap dominates (depending on the degree of mixing).

Given the high vibrational energies of organic molecules, it is unclear whether 100meV is within reach. It is however clear that not all vibrational modes couple efficiently to the electronic wavefunction (contributing to f_0), which makes the reduced effective σ_{ct} found for NFAs in our simple analysis plausible. The different coupling of vibrational modes has very recently been illustrated theoretically for C-C and C-H vibrations. Results showed that the effect of high-energy C-H vibrations on λ varied significantly from molecule to molecule.[209] It was found that C-H modes do not significantly affect λ in rubrene, explaining the lack of effect found experimentally upon deuteration of the molecule.[9] By contrast, C-H modes were found to have a strong influence for P3HT or ITIC, meaning that side-chains (containing C-H bonds) are unlikely to be benign.[209] Hetero-atoms and modifications may also help. Secondly, C-C vibrations depend on the conjugation. Thiophene, for example, has a lower ring stretching mode energy than benzene (186 vs 198meV).[210]

7. Paths forward

7.1 Comparison between trade-offs

We conclude this progress report by trying to identify paths towards higher OPV efficiency. **Figure 7** provides a simple estimate of the maximum achievable efficiencies at plausible charge generation-V_{oc} (IQE-V_{oc}) trade-offs (shown as different guidelines and obtained from the lines in **figure 6**), similar to the estimates of Baran *et al*.[164] The key assumptions are that E_g =1.6 eV, which corresponds well to the high performance NFA blends, and a flat $EQE=EQE_{max}$ in the absorption range. The *EQE* is capped at 0.95 and the *FF* set to 0.75 (*FF*

1152= 0.70 and 0.8 shown in **figure S1**). The data points are the same as those along the solid grey 1153and dashed black lines of **figure 6**. Within the guidelines, increasing the efficiency at constant 1154 can correspond to either achieving a flatter *EQE* or to decreasing the *FF-absorption* 1155trade-off. At the generation-V_{oc} values achieved by Xu *et al.*,[201] efficiencies of 16.5% are 1156within reach, provided *FF* is increased from the experimental value of 0.64 to the simulation 1157value of 0.75, and the EQE_{max} = 0.83 is made flat across the spectrum. Further reducing 1158is clearly desirable, but with the *Jsc* and *FF* values of Xu *et al.*, the efficiency achieved by 1159*fully* eliminating non-radiative recombination is only 14.5% (based on ref. [201] and = 11601.3V).

1161It should be noted that we have largely assumed the two trade-offs to be independent. This, as 1162we have discussed, is unlikely since both depend on the (non-radiative) recombination rate k_{nr}. 1163Most importantly, the trade-offs are between charge generation and V_{oc}, and between active 1164layer thickness (absorption) and charge extraction. These can only *approximately* be 1165represented with the EQE_{max}-V_{oc} and J_{sc}-*FF* metrics, because the *EQE* can be affected by 1166charge extraction and the *FF* by a field-dependent dissociation (generation-V_{oc} trade-off). For 1167example, the work of Xu *et al.*,[201] which we believe to be the state-of-the-art, shows 1168extremely high IQE_{max} and EQE_{max} but only moderate *FF*. This could be due to either a poor 1169charge extraction or a field-dependent charge generation.

1170

1171**7.2 Scientific challenges**

1172The key scientific challenges will therefore be a better understanding of the two trade-offs 1173discussed in this paper and of non-radiative recombination in OPV systems. For the former, 1174we believe new improved metrics are required. Ideally, these should both accurately reflect 1175the physics and be experimentally simple. For the latter, and NFAs in general, there remain 1176many open questions. First, what is the relative importance of intra-molecular vibrations,

inter-molecular vibrations, D-A molecular docking and environmental reorganisation in determining the non-radiative recombination rate k_{nr}? Then, how much of the EQE_{EL} improvement observed at low ΔE is caused by emission from a state with higher oscillator strength (an S_1 or S_1-CT hybrid instead of a CT state), and not by a reduced E_b^{CT}? Similarly, what is the state that recombination proceeds from at low ΔE?

3.3 New opportunities in vibrational control

Despite these unanswered questions and the preliminary nature of our analysis, the control of vibrations potentially opens a new avenue towards higher OPV efficiencies. It is interesting, for example, that of the high efficiency NFAs we analysed, the twisted perylenes used by Liu *et* al. (9.5% PCE),[119] perform the worst on the EQE_{max}-V_{oc} metric and have the highest estimated vibrational energies. The high efficiency rather stems from the other key advantage of NFAs, which is the broad *EQE* afforded by complementary donor and acceptor absorption. The main attraction of engineering vibrations is that, following the landmark work of Benduhn *et al.* on non-radiative recombination, these are understood to be intra-molecular properties, which can be more easily understood and addressed by synthesis. In contrast, it has for long been clear that high mobilities and low recombination rates are necessary, but that it is nearly impossible to link these solar cell properties to molecular structure. The analysis presented here suggests that the energy of the vibrational modes coupling to the ground and excited states can be made smaller than the 160meV benzene breathing mode. While there remain many uncertainties, engineering vibrations, such that no high-frequency modes couple to the optical gap, represents, in our opinion, a significant opportunity: It can increase the lifetime of the CT state, favouring charge separation, and reducing both the radiative and non-radiative V_{oc} losses$E_{CT}=IP_D-EA_A-\left|E_B^{CT}\right|$ and $E_B^{CT}=\frac{-q^2}{4\pi\epsilon_0\epsilon_r r_{e-h}}$. In the equilibrium non-Langevin picture, it also increases the time available for charge extraction, alleviating the *FF*-absorption

trade-off. Reducing effective vibrational energies may constitute a formidable challenge in practice. However, since the relevant vibrations are understood to correspond to those of individual molecules, it should be possible to computationally screen structures for these properties.

Supporting Information

Supporting Information is available from the Wiley Online Library or from the author.

Table S1 Values and sources of **figure 6** data

Table S2 Calculations for k_{nr}

Figure S1 Achievable efficiencies with FF =0.8 and 0.7

Figure S2 Vibronic fits used to obtain the values in **table 1**

Acknowledgements

IR thanks Dr. Bernard Wenger for useful discussions on Marcus theory and gratefully acknowledges a Doctoral Training Grant award from EPSRC. MR acknowledges funding from EPSRC (grant EP/L026066/1), from the European Union in FP 7 (grant 630864) and support from the University of Oxford. NB, MC and YZ thank the Swiss National Science Foundation (grant PP00P2_150536), the University of Bern and the University of Fribourg for financial support.

Received: ((will be filled in by the editorial staff))

Revised: ((will be filled in by the editorial staff))

Published online: ((will be filled in by the editorial staff))

References

[1] K. Kawashima, Y. Tamai, H. Ohkita, I. Osaka, K. Takimiya, *Nat. Commun.* **2015**, *6*, 10085.

[2] P. Würfel, *J. Phys. C Solid State Phys.* **1982**, *3967*.

[3] W. Tress, *Organic Solar Cells: Theory, Experiment and Device Simulations*, Springer, **2015**.

[4] U. Rau, *Phys. Rev. B* **2007**, *76*, 85303.

[5] T. M. Burke, The Device Physics of Organic Solar Cells, Stanford University, **2015**.

[6] W. Shockley, H. J. Queisser, *J. Appl. Phys.* **1961**, *32*, 510.

[7] T. Kirchartz, T. Markvart, U. Rau, D. A. Egger, **2018**, *3*.

[8] M. Sendner, P. K. Nayak, D. A. Egger, S. Beck, C. Müller, B. Epding, W. Kowalsky, L. Kronik, H. J. Snaith, A. Pucci, others, *Mater. Horizons* **2016**, *3*, 613.

[9] J. Benduhn, K. Tvingstedt, F. Piersimoni, S. Ullbrich, Y. Fan, M. Tropiano, K. A. McGarry, O. Zeika, M. K. Riede, C. J. Douglas, S. Barlow, S. R. Marder, D. Neher, D. Spoltore, K. Vandewal, *Nat. Energy* **2017**, *2*, 17053.

[10] R. T. Ross, *J. Chem. Phys.* **1967**, *46*, 4590.

[11] M. Schwoerer, H. C. Wolf, *Organic Molecular Solids*, Wiley-VCH Verlag GmbH, Weinheim, Germany, **2006**.

[12] H. Bässler, *Macromol. Symp.* **1996**, *104*, 269.

[13] H. Bässler, V. I. Arkhipov, E. V Emelianova, A. Gerhard, A. Hayer, C. Im, J. Rissler, *Synth. Met.* **2003**, *135–136*, 377.

[14] I. G. Scheblykin, A. Yartsev, T. Pullerits, V. Gulbinas, V. Sundström, *J. Phys. Chem. B* **2007**, *111*, 6303.

[15] F. Dubin, R. Melet, T. Barisien, R. Grousson, L. Legrand, M. Schott, V. Voliotis, *Nat. Phys.* **2006**, *2*, 32.

[16] N. Banerji, *J. Mater. Chem. C* **2013**, *1*, 3052.

1254[17] O. R. Tozer, W. Barford, *J. Phys. Chem. A* **2012**, *116*, 10310.

1255[18] W. Barford, I. Boczarow, T. Wharram, *J. Phys. Chem. A* **2011**, *115*, 9111.

1256[19] N. P. Wells, D. A. Blank, *Phys. Rev. Lett.* **2008**, *100*, 86403.

1257[20] A. Ruseckas, P. Wood, I. D. W. Samuel, G. R. Webster, W. J. Mitchell, P. L. Burn, V.

1258 Sundström, *Phys. Rev. B* **2005**, *72*, 115214.

1259[21] X. J. Yang, T. E. Dykstra, G. D. Scholes, *Phys. Rev. B* **2005**, *71*, 45203.

1260[22] T. E. Dykstra, V. Kovalevskij, X. J. Yang, G. D. Scholes, *Chem. Phys.* **2005**, *318*, 21.

1261[23] A. A. Bakulin, J. C. Hummelen, M. S. Pshenichnikov, P. H. M. Van Loosdrecht, *Adv.*

1262 *Funct. Mater.* **2010**, *20*, 1653.

1263[24] J.-L. Brédas, J. R. Durrant, *Acc. Chem. Res.* **2009**, *42*, 1689.

1264[25] K. Vandewal, A. Gadisa, W. D. Oosterbaan, S. Bertho, F. Banishoeib, I. Van Severen,

1265 L. Lutsen, T. J. Cleij, D. J. M. Vanderzande, J. V. Manca, *Adv. Funct. Mater.* **2008**, *18*,

1266 2064.

1267[26] R. a J. Janssen, J. Nelson, *Adv. Mater.* **2013**, *25*, 1847.

1268[27] K. C. Yee, R. R. Chance, *J. Polym. Sci. Part B Polym. Phys.* **1978**, *16*, 431.

1269[28] E. S. Maniloff, V. I. Klimov, D. W. McBranch, *Phys. Rev. B* **1997**, *56*, 1876.

1270[29] J. A. Bartelt, D. Lam, T. M. Burke, S. M. Sweetnam, M. D. McGehee, *Adv. Energy*

1271 *Mater.* **2015**, *5*, 1.

1272[30] J. Zhao, Y. Li, G. Yang, K. Jiang, H. Lin, H. Ade, W. Ma, H. Yan, *Nat. Energy* **2016**, *1*,

1273 15027.

1274[31] P. Schilinsky, C. Waldauf, C. J. Brabec, *Appl. Phys. Lett.* **2002**, *81*, 3885.

1275[32] G. Zhao, Y. He, Y. Li, *Adv. Mater.* **2010**, *22*, 4355.

1276[33] M. Causa', J. De Jonghe-Risse, M. Scarongella, J. C. Brauer, E. Buchaca-Domingo, J.

1277 E. Moser, N. Stingelin, N. Banerji, *Nat. Commun.* **2016**, *7*, 12556.

1278[34] M. Scarongella, J. De Jonghe-Risse, E. Buchaca-Domingo, M. Causa', Z. Fei, M.

1279 Heeney, J. E. Moser, N. Stingelin, N. Banerji, *J. Am. Chem. Soc.* **2015**, *137*, 2908.

1280[35] F. C. Jamieson, E. B. Domingo, T. McCarthy-Ward, M. Heeney, N. Stingelin, J. R.
1281 Durrant, *Chem. Sci.* **2012**, *3*, 485.
1282[36] A. C. Mayer, M. F. Toney, S. R. Scully, J. Rivnay, C. J. Brabec, M. Scharber, M.
1283 Koppe, M. Heeney, I. McCulloch, M. D. Mcgehee, *Adv. Funct. Mater.* **2009**, *19*, 1173.
1284[37] Z. He, B. Xiao, F. Liu, H. Wu, Y. Yang, S. Xiao, C. Wang, T. P. Russell, Y. Cao, *Nat.*
1285 *Photonics* **2015**, *9*, 174.
1286[38] L. Lu, L. Yu, *Adv. Mater.* **2014**, *26*, 4413.
1287[39] J. M. Szarko, B. S. Rolczynski, S. J. Lou, T. Xu, J. Strzalka, T. J. Marks, L. Yu, L. X.
1288 Chen, *Adv. Funct. Mater.* **2014**, *24*, 10.
1289[40] Y. Liu, J. Zhao, Z. Li, C. Mu, W. Ma, H. Hu, K. Jiang, H. Lin, H. Ade, H. Yan, *Nat.*
1290 *Commun.* **2014**, *5*, 5293.
1291[41] K. H. Hendriks, W. Li, G. H. L. Heintges, G. W. P. Van Pruissen, M. M. Wienk, R. A.
1292 J. Janssen, *J. Am. Chem. Soc.* **2014**, *136*, 11128.
1293[42] T. Vangerven, P. Verstappen, J. Drijkoningen, W. Dierckx, S. Himmelberger, A. Salleo,
1294 D. J. M. Vanderzande, W. Maes, J. V. Manca, *Chem. Mater.* **2015**, *27*, 3726.
1295[43] M. K. Riede, T. Mueller, W. Tress, R. Schueppel, K. Leo, *Nanotechnology* **2008**, *19*,
1296 424001.
1297[44] S. Pfuetzner, J. Meiss, A. Petrich, M. K. Riede, K. Leo, *Appl. Phys. Lett.* **2009**, *94*,
1298 253303.
1299[45] P. Peumans, S. Uchida, S. R. Forrest, *Nature* **2003**, *425*, 158.
1300[46] R. Fitzner, E. Reinold, A. Mishra, E. Mena-Osteritz, H. Ziehlke, C. Körner, K. Leo, M.
1301 K. Riede, M. Weil, O. Tsaryova, A. Weiß, C. Uhrich, M. Pfeiffer, P. Bäuerle, *Adv.*
1302 *Funct. Mater.* **2011**, *21*, 897.
1303[47] R. Schueppel, K. Schmidt, C. Uhrich, K. Schulze, D. Wynands, J.-L. Brédas, E. Brier,
1304 E. Reinold, H. B. Bu, P. Baeuerle, B. Maennig, M. Pfeiffer, K. Leo, *Phys. Rev. B* **2008**,
1305 *77*, 1.

1306[48] G. Chen, H. Sasabe, Z. Wang, X. Wang, Z. Hong, J. Kido, Y. Yang, *Phys. Chem.*
1307 *Chem. Phys.* **2012**, *14*, 14661.
1308[49] O. L. Griffith, X. Liu, J. A. Amonoo, P. I. Djurovich, M. E. Thompson, P. F. Green, S.
1309 R. Forrest, *Phys. Rev. B - Condens. Matter Mater. Phys.* **2015**, *92*, 1.
1310[50] S. D. Collins, N. A. Ran, M. C. Heiber, T.-Q. Nguyen, *Adv. Energy Mater.* **2017**, *7*,
1311 1602242.
1312[51] W. Zhao, S. Li, H. Yao, S. Zhang, Y. Zhang, B. Yang, J. Hou, *J. Am. Chem. Soc.* **2017**,
1313 *139*, 7148.
1314[52] K. Vandewal, K. Tvingstedt, A. Gadisa, O. Inganäs, J. V. Manca, *Nat. Mater.* **2009**, *8*,
1315 904.
1316[53] K. Tvingstedt, K. Vandewal, A. Gadisa, F. Zhang, J. V. Manca, O. Inganäs, *J. Am.*
1317 *Chem. Soc.* **2009**, *131*, 11819.
1318[54] K. Vandewal, K. Tvingstedt, A. Gadisa, O. Inganäs, J. V. Manca, *Phys. Rev. B* **2010**,
1319 *81*, 125204.
1320[55] K. Vandewal, S. Albrecht, E. T. Hoke, K. R. Graham, J. Widmer, J. D. Douglas, M.
1321 Schubert, W. R. Mateker, J. T. Bloking, G. F. Burkhard, A. Sellinger, J. M. J. Fréchet,
1322 A. Amassian, M. K. Riede, M. D. McGehee, D. Neher, A. Salleo, *Nat. Mater.* **2014**, *13*,
1323 63.
1324[56] G. Grancini, M. Maiuri, D. Fazzi, A. Petrozza, H.-J. Egelhaaf, D. Brida, G. Cerullo, G.
1325 Lanzani, *Nat. Mater.* **2013**, *12*, 29.
1326[57] A. Armin, Y. Zhang, P. L. Burn, P. Meredith, A. Pivrikas, *Nat. Mater.* **2013**, *12*, 594.
1327[58] M. C. Scharber, *Nat. Mater.* **2013**, *12*, 593.
1328[59] K. Vandewal, J. Benduhn, K. S. Schellhammer, T. Vangerven, J. E. Rückert, F.
1329 Piersimoni, R. Scholz, O. Zeika, Y. Fan, S. Barlow, D. Neher, S. R. Marder, J. V.
1330 Manca, D. Spoltore, G. Cuniberti, F. Ortmann, *J. Am. Chem. Soc.* **2017**, *139*, 1699.
1331[60] T. M. Burke, S. M. Sweetnam, K. Vandewal, M. D. Mcgehee, *Adv. Energy Mater.*

2015, 1500123.

[61] T. M. Clarke, J. R. Durrant, *Chem. Rev.* **2010**, *110*, 6736.

[62] V. I. Arkhipov, P. Heremans, H. Bässler, *Appl. Phys. Lett.* **2003**, *82*, 4605.

[63] S. M. Ryno, M. K. Ravva, X. Chen, H. Li, J.-L. Brédas, *Adv. Energy Mater.* **2016**, DOI 10.1002/aenm.201600568.

[64] A. Salleo, R. J. Kline, D. M. DeLongchamp, M. L. Chabinyc, *Adv. Mater.* **2010**, *22*, 3812.

[65] C. J. Brabec, M. Heeney, I. McCulloch, J. Nelson, *Chem. Soc. Rev.* **2011**, *40*, 1185.

[66] B. A. Collins, J. R. Tumbleston, H. Ade, *J. Phys. Chem. Lett.* **2011**.

[67] D. M. DeLongchamp, R. J. Kline, A. Herzing, *Energy Environ. Sci.* **2012**, *5*, 5980.

[68] P. Müller-Buschbaum, *Adv. Mater.* **2014**, 7692.

[69] F. Padinger, R. S. Rittberger, N. S. Sariciftci, *Adv. Funct. Mater.* **2003**, *13*, 85.

[70] G. Li, Y. Yao, H. Yang, V. Shrotriya, G. Yang, Y. Yang, *Adv. Funct. Mater.* **2007**, *17*, 1636.

[71] F. Zhang, K. G. Jespersen, C. Björström, M. Svensson, M. R. Andersson, V. Sundström, K. Magnusson, E. Moons, A. Yartsev, O. Inganäs, *Adv. Funct. Mater.* **2006**, *16*, 667.

[72] J. Peet, J. Y. Kim, N. E. Coates, W. L. Ma, D. Moses, A. J. Heeger, G. C. Bazan, *Nat. Mater.* **2007**, *6*, 497.

[73] J. Yang, D. Yan, T. S. Jones, *Chem. Rev.* **2015**, *115*, 5570.

[74] R. Fitzner, E. Mena-Osteritz, A. Mishra, G. Schulz, E. Reinold, M. Weil, C. Körner, H. Ziehlke, C. Elschner, K. Leo, M. K. Riede, M. Pfeiffer, C. Uhrich, P. Bäuerle, *J. Am. Chem. Soc.* **2012**, *134*, 11064.

[75] K. R. Graham, C. Cabanetos, J. P. Jahnke, M. N. Idso, A. El Labban, G. O. Ngongang Ndjawa, T. Heumueller, K. Vandewal, A. Salleo, B. F. Chmelka, A. Amassian, P. M. Beaujuge, M. D. McGehee, *J. Am. Chem. Soc.* **2014**, *136*, 9608.

1358[76] A. M. Hiszpanski, Y.-L. Loo, *Energy Environ. Sci.* **2014**, *7*, 592.

1359[77] N. D. Treat, J. A. N. Malik, O. Reid, L. Yu, C. G. Shuttle, G. Rumbles, C. J. Hawker,

1360 M. L. Chabinyc, P. Smith, N. Stingelin, *Nat. Mater.* **2013**, *12*, 628.

1361[78] S. Lan, H. Yang, G. Zhang, X. Wu, W. Ning, S. Wang, H. Chen, T. Guo, *J. Phys.*

1362 *Chem. C* **2016**, acs. jpcc.6b08025.

1363[79] Z. He, C. Zhong, S. Su, M. Xu, H. Wu, Y. Cao, *Nat. Photonics* **2012**, *6*, 591.

1364[80] R. Pandey, R. J. Holmes, *Adv. Mater.* **2010**, *22*, 5301.

1365[81] B. A. Collins, Z. Li, J. R. Tumbleston, E. Gann, C. R. McNeill, H. Ade, *Adv. Energy*

1366 *Mater.* **2013**, *3*, 65.

1367[82] J. a. Bartelt, Z. M. Beiley, E. T. Hoke, W. R. Mateker, J. D. Douglas, B. A. Collins, J.

1368 R. Tumbleston, K. R. Graham, A. Amassian, H. Ade, J. M. J. Fréchet, M. F. Toney, M.

1369 D. McGehee, *Adv. Energy Mater.* **2013**, *3*, 364.

1370[83] B. Watts, W. J. Belcher, L. Thomsen, H. Ade, P. C. Dastoor, *Macromolecules* **2009**, *42*,

1371 8392.

1372[84] R. Banerjee, J. Novak, C. Frank, C. Lorch, A. Hinderhofer, A. Gerlach, F. Schreiber,

1373 *Phys. Rev. Lett.* **2013**, *110*, 1.

1374[85] T. M. Burke, M. D. McGehee, *Adv. Mater.* **2014**, *26*, 1923.

1375[86] N. C. Miller, E. Cho, M. J. N. Junk, R. Gysel, C. Risko, D. Kim, S. M. Sweetnam, C.

1376 E. Miller, L. J. Richter, R. J. Kline, M. Heeney, I. McCulloch, A. Amassian, D.

1377 Acevedo-Feliz, C. Knox, M. R. Hansen, D. Dudenko, B. F. Chmelka, M. F. Toney, J.-

1378 L. Brédas, M. D. McGehee, *Adv. Mater.* **2012**, *24*, 6071.

1379[87] W. Li, K. H. Hendriks, A. Furlan, M. M. Wienk, R. A. J. Janssen, *J. Am. Chem. Soc.*

1380 **2015**, *137*, 2231.

1381[88] H. Ohkita, S. Cook, Y. Astuti, W. Duffy, S. Tierney, W. Zhang, M. Heeney, I.

1382 McCulloch, J. Nelson, D. D. C. Bradley, J. R. Durrant, *J. Am. Chem. Soc.* **2008**, *130*,

1383 3030.

1384[89] T. M. Clarke, A. M. Ballantyne, J. Nelson, D. D. C. Bradley, J. R. Durrant, *Adv. Funct.*
1385 *Mater.* **2008**, *18*, 4029.
1386[90] A. A. Bakulin, A. Rao, V. G. Pavelyev, P. H. M. Van Loosdrecht, M. S. Pshenichnikov,
1387 D. Niedzialek, J. Cornil, D. Beljonne, R. H. Friend, *Science (80-.).* **2012**, *335*, 1340.
1388[91] A. E. Jailaubekov, A. P. Willard, J. R. Tritsch, W.-L. Chan, N. Sai, R. Gearba, L. G.
1389 Kaake, K. J. Williams, K. Leung, P. J. Rossky, X.-Y. Zhu, *Nat. Mater.* **2013**, *12*, 66.
1390[92] P. A. Lane, P. D. Cunningham, J. S. Melinger, O. Esenturk, E. J. Heilweil, *Nat.*
1391 *Commun.* **2015**, *6*, 7558.
1392[93] F. Provencher, N. Bérubé, A. W. Parker, G. M. Greetham, M. Towrie, C. Hellmann, M.
1393 Côté, N. Stingelin, C. Silva, S. C. Hayes, *Nat. Commun.* **2014**, *5*, 4288.
1394[94] I. A. Howard, F. Etzold, F. Laquai, M. Kemerink, *Adv. Energy Mater.* **2014**, *4*,
1395 1301743.
1396[95] B. R. Gautam, R. Younts, W. Li, L. Yan, E. Danilov, E. Klump, I. Constantinou, F. So,
1397 W. You, H. Ade, K. Gundogdu, *Adv. Energy Mater.* **2016**, *6*, 1.
1398[96] M. Tabachnyk, S. L. Smith, L. R. Weiss, A. Sadhanala, A. W. Chin, R. H. Friend, A.
1399 Rao, *arXiv* **2017**, 1.
1400[97] J. Lee, K. Vandewal, S. R. Yost, M. E. Bahlke, L. Goris, M. A. Baldo, J. V. Manca, T.
1401 Van Voorhis, *J. Am. Chem. Soc.* **2010**, *132*, 11878.
1402[98] D. H. K. Murthy, A. Melianas, Z. Tang, G. Juška, K. Arlauskas, F. Zhang, L. D. a.
1403 Siebbeles, O. Inganäs, T. J. Savenije, *Adv. Funct. Mater.* **2013**, *23*, 4262.
1404[99] C. L. Braun, *J. Chem. Phys.* **1984**, *80*, 4157.
1405[100] J. M. Hodgkiss, S. Albert-Seifried, A. Rao, A. J. Barker, A. R. Campbell, R. A. Marsh,
1406 R. H. Friend, *Adv. Funct. Mater.* **2012**, *22*, 1567.
1407[101] P. Langevin, *Ann. Chim. Phys.* **1903**, *28*, 433.
1408[102] A. Rao, P. C. Y. Chow, S. Gélinas, C. W. Schlenker, C.-Z. Li, H.-L. Yip, A. K. Y. Jen,
1409 D. S. Ginley, R. H. Friend, *Nature* **2013**, *500*, 435.

1410[103] W. Tress, K. Leo, M. K. Riede, *Phys. Rev. B* **2012**, *85*, 155201.

1411[104] M. H. Chang, M. J. Frampton, H. L. Anderson, L. M. Herz, *Phys. Rev. Lett.* **2007**, *98*, 1.

1412[105] S. Gélinas, A. Rao, A. Kumar, S. L. Smith, A. W. Chin, J. Clark, T. S. van der Poll, G.
1413 C. Bazan, R. H. Friend, *Science (80-.).* **2014**, *343*, 512.

1414[106] C. S. Ponseca, A. Yartsev, E. Wang, M. R. Andersson, D. A. Vithanage, V. Sundström,
1415 *J. Am. Chem. Soc.* **2012**, *134*, 11836.

1416[107] X. Ai, M. C. Beard, K. P. Knutsen, S. E. Shaheen, G. Rumbles, R. J. Ellingson, *J. Phys.*
1417 *Chem. B* **2006**, *110*, 25462.

1418[108] D. Veldman, Ö. Ipek, S. C. J. Meskers, J. Sweelssen, M. M. Koetse, S. C. Veenstra, J.
1419 M. Kroon, S. S. Van Bavel, J. Loos, R. A. J. Janssen, *J. Am. Chem. Soc.* **2008**, *130*,
1420 7721.

1421[109] P. Pingel, A. Zen, R. D. Abellón, F. C. Grozema, L. D. A. Siebbeles, D. Neher, *Adv.*
1422 *Funct. Mater.* **2010**, *20*, 2286.

1423[110] C. J. Brabec, G. Zerza, G. Cerullo, S. De Silvestri, S. Luzzati, J. C. Hummelen, S.
1424 Sariciftci, *Chem. Phys. Lett.* **2001**, *340*, 232.

1425[111] A. C. Jakowetz, M. L. Böhm, J. Zhang, A. Sadhanala, S. Huettner, A. A. Bakulin, A.
1426 Rao, R. H. Friend, *J. Am. Chem. Soc.* **2016**, *138*, 11672.

1427[112] S. M. Falke, C. A. Rozzi, D. Brida, M. Maiuri, M. Amato, E. Sommer, A. De Sio, A.
1428 Rubio, G. Cerullo, E. Molinari, C. Lienau, others, *Science (80-.).* **2014**, *344*, 1001.

1429[113] Y. Song, S. N. Clafton, R. D. Pensack, T. W. Kee, G. D. Scholes, *Nat. Commun.* **2014**,
1430 *5*, DOI Artn 4933Doi 10.1038/Ncomms5933.

1431[114] A. J. Barker, K. Chen, J. M. Hodgkiss, *J. Am. Chem. Soc.* **2014**, *136*, 12018.

1432[115] I. A. Howard, R. Mauer, M. Meister, F. Laquai, *J. Am. Chem. Soc.* **2010**, *132*, 14866.

1433[116] A. Zusan, **2014**.

1434[117] A. Armin, M. Velusamy, P. Wolfer, Y. Zhang, P. L. Burn, P. Meredith, A. Pivrikas,
1435 *ACS Photonics* **2014**, *1*, 173.

1436[118] B. M. Savoie, A. Rao, A. A. Bakulin, S. Gélinas, B. Movaghar, R. H. Friend, T. J.
1437 Marks, M. A. Ratner, *J. Am. Chem. Soc.* **2014**, *136*, 2876.
1438[119] J. Liu, S. Chen, D. Qian, B. R. Gautam, G. Yang, J. Zhao, J. Bergqvist, F. Zhang, W.
1439 Ma, H. Ade, O. Inganäs, K. Gundogdu, F. Gao, H. Yan, *Nat. Energy* **2016**, *1*, 16089.
1440[120] S. Verlaak, D. Beljonne, D. Cheyns, C. Rolin, M. Linares, F. Castet, J. Cornil, P.
1441 Heremans, *Adv. Funct. Mater.* **2009**, *19*, 3809.
1442[121] M. Linares, D. Beljonne, J. Cornil, K. Lancaster, J.-L. Brédas, S. Verlaak, A.
1443 Mityashin, P. Heremans, A. Fuchs, C. Lennartz, J. Idé, R. Méreau, P. Aurel, L.
1444 Ducasse, F. Castet, *J. Phys. Chem. C* **2010**, *114*, 3215.
1445[122] J. Idé, S. Mothy, A. Savoyant, A. Fritsch, P. Aurel, R. Méreau, L. Ducasse, J. Cornil,
1446 D. Beljonne, F. Castet, *Int. J. Quantum Chem.* **2013**, *113*, 580.
1447[123] S. M. Ryno, Y. T. Fu, C. Risko, J.-L. Brédas, *ACS Appl. Mater. Interfaces* **2016**, *8*,
1448 15524.
1449[124] S. R. Yost, T. Van Voorhis, *J. Phys. Chem. C* **2013**, *117*, 5617.
1450[125] S. Duhm, G. Heimel, I. Salzmann, H. Glowatzki, R. L. Johnson, A. Vollmer, J. P. Rabe,
1451 N. Koch, *Nat. Mater.* **2008**, *7*, 326.
1452[126] A. Ojala, A. Petersen, A. Fuchs, R. Lovrincic, C. P??lking, J. Trollmann, J. Hwang, C.
1453 Lennartz, H. Reichelt, H. W. H??ffken, A. Pucci, P. Erk, T. Kirchartz, F. Würthner,
1454 *Adv. Funct. Mater.* **2012**, *22*, 86.
1455[127] B. P. Rand, D. Cheyns, K. Vasseur, N. C. Giebink, S. Mothy, Y. Yi, V. Coropceanu, D.
1456 Beljonne, J. Cornil, J.-L. Brédas, J. Genoe, *Adv. Funct. Mater.* **2012**, *22*, 2987.
1457[128] X. Liu, K. Ding, A. Panda, S. R. Forrest, *ACS Nano* **2016**, *10*, 7619.
1458[129] A. N. Brigeman, M. A. Fusella, Y. Yan, G. E. Purdum, Y.-L. Loo, B. P. Rand, N. C.
1459 Giebink, *Adv. Energy Mater.* **2016**, 1601001.
1460[130] G. O. N. Ndjawa, K. R. Graham, S. Mollinger, D. M. Wu, D. Hanifi, R. Prasanna, B.
1461 D. Rose, S. Dey, L. Yu, J.-L. Brédas, M. D. McGehee, A. Salleo, A. Amassian, *Adv.*

1462 *Energy Mater.* **2017**, 1601995.

1463[131] K. R. Graham, G. O. N. Ndjawa, S. M. Conron, R. Munir, K. Vandewal, J. J. Chen, S.

1464 M. Sweetnam, M. E. Thompson, A. Salleo, M. D. Mcgehee, A. Amassian, *Adv. Energy*

1465 *Mater.* **2016**, 1.

1466[132] M. L. Tietze, W. Tress, S. Pfützner, C. Schünemann, L. Burtone, M. K. Riede, K. Leo,

1467 K. Vandewal, S. S. Olthof, P. Schulz, A. Kahn, *Phys. Rev. B* **2013**, *88*, 1.

1468[133] S. Mollinger, K. Vandewal, A. Salleo, *Adv. Energy Mater.* **2015**, *5*, 1.

1469[134] J. R. Tumbleston, B. A. Collins, L. Yang, A. C. Stuart, E. Gann, W. Ma, W. You, H.

1470 Ade, *Nat. Photonics* **2014**, *1*, 1.

1471[135] N. A. Ran, J. A. Love, C. J. Takacs, A. Sadhanala, J. K. Beavers, S. D. Collins, Y.

1472 Huang, M. Wang, R. H. Friend, G. C. Bazan, T. Q. Nguyen, *Adv. Mater.* **2016**, *28*,

1473 1482.

1474[136] B. A. Gregg, *MRS Bull.* **2005**, *30*, 20.

1475[137] B. A. Gregg, *J. Phys. Chem. Lett.* **2011**, *2*, 3013.

1476[138] S. N. Hood, I. Kassal, *J. Phys. Chem. Lett.* **2016**, *7*, 4495.

1477[139] D. B. Sulas, K. Yao, J. J. Intemann, S. T. Williams, C. Z. Li, C. C. Chueh, J. J.

1478 Richards, Y. Xi, L. D. Pozzo, C. W. Schlenker, A. K. Y. Jen, D. S. Ginley, *Chem.*

1479 *Mater.* **2015**, *27*, 6583.

1480[140] C. Deibel, T. Strobel, V. Dyakonov, *Phys. Rev. Lett.* **2009**, *103*, 1.

1481[141] C. Groves, *Energy Environ. Sci.* **2013**, *6*, 3202.

1482[142] D. A. Vithanage, A. Devižis, V. Abramavičius, Y. Infahsaeng, R. C. I. MacKenzie, P.

1483 E. Keivanidis, A. Yartsev, D. Hertel, J. Nelson, V. Sundström, V. Gulbinas, *Nat.*

1484 *Commun.* **2013**, *4*, 2334.

1485[143] N. R. Monahan, K. W. Williams, B. Kumar, C. Nuckolls, X. Y. Zhu, *Phys. Rev. Lett.*

1486 **2015**, *114*, 1.

1487[144] T. Kirchartz, K. Taretto, U. Rau, *J. Phys. Chem. C* **2009**, *113*, 17958.

1488[145] M. Gruber, J. Wagner, K. Klein, U. Hörmann, A. Opitz, M. Stutzmann, W. Brütting,
1489 *Adv. Energy Mater.* **2012**, *2*, 1100.
1490[146] G. Garcia-Belmonte, *Sol. Energy Mater. Sol. Cells* **2010**, *94*, 2166.
1491[147] T. Kirchartz, F. Deledalle, P. S. Tuladhar, J. R. Durrant, J. Nelson, *J. Phys. Chem. Lett.*
1492 **2013**, *4*, 2371.
1493[148] G. J. Adriaenssens, V. I. Arkhipov, *Solid State Commun.* **1997**, *103*, 541.
1494[149] A. Pivrikas, A. J. Mozer, G. Juška, M. Scharber, K. Arlauskas, N. S. Sariciftci, H.
1495 Stubb, R. Österbacka, *Phys. Rev. Lett.* **2005**, *94*, 1.
1496[150] L. J. A. Koster, V. D. Mihailetchi, P. W. M. Blom, *Appl. Phys. Lett.* **2006**, *88*, 52104.
1497[151] M. Nyman, O. J. Sandberg, R. Österbacka, *Adv. Energy Mater.* **2015**, *5*, n/a.
1498[152] M. C. Heiber, C. Baumbach, V. Dyakonov, C. Deibel, *Phys. Rev. Lett.* **2015**, *114*, 1.
1499[153] C. Deibel, a. Wagenpfahl, V. Dyakonov, *Phys. Rev. B* **2009**, *80*, 1.
1500[154] M. Hilczer, M. Tachiya, *J. Phys. Chem. C* **2010**, *114*, 6808.
1501[155] T. Kirchartz, J. Nelson, *Phys. Rev. B* **2012**, *86*, 165201.
1502[156] F. Deledalle, P. S. Tuladhar, J. Nelson, J. R. Durrant, T. Kirchartz, *J. Phys. Chem. C*
1503 **2014**, *118*, 8837.
1504[157] M. Stolterfoht, A. Armin, S. Shoaee, I. Kassal, P. L. Burn, P. Meredith, *Nat. Commun.*
1505 **2016**, *7*, 11944.
1506[158] A. C. Jakowetz, M. L. Böhm, A. Sadhanala, S. Huettner, A. Rao, R. H. Friend, *Nat.*
1507 *Mater.* **2017**, DOI 10.1038/NMAT4865.
1508[159] Y. Liu, K. Zojer, B. Lassen, J. Kjelstrup-Hansen, H. G. Rubahn, M. V. Madsen, *J. Phys.*
1509 *Chem. C* **2015**, *119*, 26588.
1510[160] L. J. A. Koster, S. E. Shaheen, J. C. Hummelen, *Adv. Energy Mater.* **2012**, *2*, 1246.
1511[161] S. Chen, S. W. Tsang, T. H. Lai, J. R. Reynolds, F. So, *Adv. Mater.* **2014**, 6125.
1512[162] N. Cho, C. W. Schlenker, K. M. Knesting, P. Koelsch, H. L. Yip, D. S. Ginley, A. K. Y.
1513 Jen, *Adv. Energy Mater.* **2014**, *4*, DOI 10.1002/aenm.201301857.

1514[163] S. Y. Leblebici, T. L. Chen, P. Olalde-Velasco, W. Yang, B. Ma, *ACS Appl. Mater.*
1515 *Interfaces* **2013**, *5*, 10105.
1516[164] D. Baran, T. Kirchartz, S. Wheeler, S. Dimitrov, M. Abdelsamie, J. Gorman, R. Ashraf,
1517 S. Holliday, A. Wadsworth, N. Gasparini, P. Kaienburg, H. Yan, A. Amassian, C. J.
1518 Brabec, J. R. Durrant, I. McCulloch, *Energy Environ. Sci.* **2016**, *9*, 3783.
1519[165] W. Tress, K. Leo, M. K. Riede, *Appl. Phys. Lett.* **2013**, *102*, 163901.
1520[166] D. Bartesaghi, I. del C. Pérez, J. Kniepert, S. Roland, M. Turbiez, D. Neher, L. J. A.
1521 Koster, *Nat. Commun.* **2015**, *6*, 7083.
1522[167] Z. Tang, B. Liu, A. Melianas, J. Bergqvist, W. Tress, Q. Bao, D. Qian, O. Inganäs, F.
1523 Zhang, *Adv. Mater.* **2015**, *27*, 1900.
1524[168] N. Gasparini, L. Lucera, M. Salvador, M. Prosa, G. D. Spyropoulos, P. Kubis, H.-J.
1525 Egelhaaf, C. J. Brabec, T. Ameri, *Energy Environ. Sci.* **2017**, *10*, 885.
1526[169] U. Würfel, D. Neher, A. Spies, S. Albrecht, *Nat. Commun.* **2015**, *6*, 6951.
1527[170] K. Tvingstedt, C. Deibel, *Adv. Energy Mater.* **2016**, *6*, 1.
1528[171] C. M. Proctor, J. A. Love, T. Q. Nguyen, *Adv. Mater.* **2014**, *26*, 5957.
1529[172] X. Xiao, K. J. Bergemann, J. D. Zimmerman, K. Lee, S. R. Forrest, *Adv. Energy Mater.*
1530 **2014**, *4*, 1301557.
1531[173] M. Zhang, H. Wang, H. Tian, Y. Geng, C. W. Tang, *Adv. Mater.* **2011**, *23*, 4960.
1532[174] B. Yang, F. Guo, Y. Yuan, Z. Xiao, Y. Lu, Q. Dong, J. Huang, *Adv. Mater.* **2013**, *25*,
1533 572.
1534[175] K. Vandewal, J. Widmer, T. Heumueller, C. J. Brabec, M. D. McGehee, K. Leo, M. K.
1535 Riede, A. Salleo, *Adv. Mater.* **2014**, *26*, 3839.
1536[176] B. Bernardo, D. Cheyns, B. Verreet, R. D. Schaller, B. P. Rand, N. C. Giebink, *Nat.*
1537 *Commun.* **2014**, *5*, 3245.
1538[177] Y. Zheng, W. J. Potscavage, T. Komino, M. Hirade, J. Adachi, C. Adachi, *Appl. Phys.*
1539 *Lett.* **2013**, *102*, 143304.

1540[178] Y. Zheng, W. J. Potscavage, T. Komino, C. Adachi, *Appl. Phys. Lett.* **2013**, *102*,
1541 153302.
1542[179] W. J. Potscavage, S. Yoo, B. Kippelen, *Appl. Phys. Lett.* **2008**, *93*, 193308.
1543[180] X. Chen, M. K. Ravva, H. Li, S. M. Ryno, J. Brédas, *Adv. Energy Mater.* **2016**, *6*.
1544[181] A. Melianas, V. Pranculis, D. Spoltore, J. Benduhn, O. Inganäs, V. Gulbinas, K.
1545 Vandewal, M. Kemerink, *Adv. Energy Mater.* **2017**, *1700888*, 1700888.
1546[182] Y. Lin, J. Wang, Z.-G. Zhang, H. Bai, Y. Li, D. Zhu, X. Zhan, *Adv. Mater.* **2015**, *27*,
1547 1170.
1548[183] Y. Yang, Z. G. Zhang, H. Bin, S. Chen, L. Gao, L. Xue, C. Yang, Y. Li, *J. Am. Chem.*
1549 *Soc.* **2016**, *138*, 15011.
1550[184] Y. Li, X. Liu, F.-P. Wu, Y. Zhou, Z.-Q. Jiang, B. Song, Y. Xia, Z.-G. Zhang, F. Gao, O.
1551 Inganäs, Y. Li, L.-S. Liao, *J. Mater. Chem. A* **2016**, *4*, 5890.
1552[185] Y. Zhong, M. T. Trinh, R. Chen, G. E. Purdum, P. P. Khlyabich, M. Sezen, S. Oh, H.
1553 Zhu, B. Fowler, B. Zhang, W. Wang, C.-Y. Nam, M. Y. Sfeir, C. T. Black, M. L.
1554 Steigerwald, Y.-L. Loo, F. Ng, X.-Y. Zhu, C. Nuckolls, *Nat. Commun.* **2015**, *6*, 8242.
1555[186] Z. Zheng, O. M. Awartani, B. R. Gautam, D. Liu, Y. Qin, W. Li, A. Bataller, K.
1556 Gundogdu, H. Ade, J. Hou, *Adv. Mater.* **2016**, 3.
1557[187] W. Zhao, S. Li, H. Yao, S. Zhang, Y. Zhang, B. Yang, J. Hou, *J. Am. Chem. Soc.* **2017**,
1558 *139*, 7148.
1559[188] a. M. Rao, P. Zhou, K. a Wang, G. T. Hager, J. M. Holden, Y. Wang, W. T. Lee, X. X.
1560 Bi, P. C. Eklund, D. S. Cornett, M. A. Duncan, I. J. Amster, *Science (80-.).* **1993**, *259*,
1561 955.
1562[189] A. Distler, The Role of Fullerenes in the Photo-Degradation of Organic Solar Cells,
1563 Friedrich-Alexander-Universität Erlangen-Nürnberg, **2015**.
1564[190] T. Heumueller, W. R. Mateker, A. Distler, U. F. Fritze, R. Cheacharoen, W. H. Nguyen,
1565 M. Biele, M. Salvador, M. von Delius, H.-J. Egelhaaf, M. D. McGehee, C. J. Brabec,

1566 *Energy Environ. Sci.* **2015**, *9*, 247.

1567[191] H. Cha, J. Wu, A. Wadsworth, J. Nagitta, S. Limbu, S. Pont, Z. Li, J. Searle, M. F.

1568 Wyatt, D. Baran, J. S. Kim, I. McCulloch, J. R. Durrant, *Adv. Mater.* **2017**, *29*, 1.

1569[192] S. Holliday, R. S. Ashraf, A. Wadsworth, D. Baran, S. A. Yousaf, C. B. Nielsen, C. H.

1570 Tan, S. D. Dimitrov, Z. Shang, N. Gasparini, M. Alamoudi, F. Laquai, C. J. Brabec, A.

1571 Salleo, J. R. Durrant, I. McCulloch, *Nat. Commun.* **2016**, *7*, 1.

1572[193] G. Han, Y. Guo, X. Song, Y. Wang, Y. Yi, *J. Mater. Chem. C* **2017**, *5*, 4852.

1573[194] F. Yang, D. Qian, A. H. Balawi, Y. Wu, W. Ma, F. Laquai, Z. Tang, F. Zhang, W. Li,

1574 *Phys. Chem. Chem. Phys.* **2017**, *19*, 23990.

1575[195] E. T. Hoke, K. Vandewal, J. A. Bartelt, W. R. Mateker, J. D. Douglas, R. Noriega, K.

1576 R. Graham, J. M. J. Fréchet, A. Salleo, M. D. Mcgehee, *Adv. Energy Mater.* **2013**, *3*,

1577 220.

1578[196] N. D. Eastham, J. L. Logsdon, E. F. Manley, T. J. Aldrich, M. J. Leonardi, G. Wang, N.

1579 E. Powers-Riggs, R. M. Young, L. X. Chen, M. R. Wasielewski, F. S. Melkonyan, R. P.

1580 H. Chang, T. J. Marks, *Adv Mater* **2018**, *30*, DOI 10.1002/adma.201704263.

1581[197] Z. Zheng, O. M. Awartani, B. Gautam, D. Liu, Y. Qin, W. Li, A. Bataller, K.

1582 Gundogdu, H. Ade, J. Hou, *Adv Mater* **2017**, *29*, DOI 10.1002/adma.201604241.

1583[198] Y. Li, L. Zhong, B. Gautam, H.-J. Bin, J.-D. Lin, F.-P. Wu, Z. Zhang, Z.-Q. Jiang, Z.-

1584 G. Zhang, K. Gundogdu, Y. Li, L.-S. Liao, *Energy Environ. Sci.* **2017**, *10*, 1610.

1585[199] K. H. Hendriks, A. S. G. Wijpkema, J. J. Van Franeker, M. M. Wienk, R. A. J. Janssen,

1586 *J. Am. Chem. Soc.* **2016**, *138*, 10026.

1587[200] W. Li, W. S. C. Roelofs, M. M. Wienk, R. A. J. Janssen, *J. Am. Chem. Soc.* **2012**, *134*,

1588 13787.

1589[201] X. Xu, T. Yu, Z. Bi, W. Ma, Y. Li, Q. Peng, *Adv. Mater.* **2017**, *1703973*, 1703973.

1590[202] S. Kazaoui, N. Minami, Y. Tanabe, H. J. Byrne, A. Eilmes, P. Petelenz, *Phys. Rev. B*

1591 **1998**, *58*, 7689.

1592[203] A. Köhler, H. Bässler, *Electronic Processes in Organic Semiconductors: An*
1593 *Introduction*, Wiley-VCH Verlag GmbH, **2015**.
1594[204] I. R. Gould, S. Farid, D. Noukakis, J. L. Goodman, R. H. Young, *J. Am. Chem. Soc.*
1595 **1993**, *115*, 3830.
1596[205] J. Ulstrup, J. Jortner, *J. Chem. Phys.* **1975**, *63*, 4358.
1597[206] M. Bixon, J. Jortner, J. W. Verhoeven, *J. Am. Chem. Soc.* **1994**, *116*, 7349.
1598[207] R. Englman, J. Jortner, *J. Lumin.* **1970**, *1–2*, 134.
1599[208] F. C. Spano, *Acc. Chem. Res.* **2009**, *43*, 429.
1600[209] X. K. Chen, J.-L. Brédas, *Adv. Energy Mater.* **2017**, *1702227*, 1.
1601[210] T. Shimanouchi, *J. Phys. Chem. Ref. Data* **1972**, *1*, 189.
1602[211] Y.-H. Chen, L.-Y. Lin, C.-W. Lu, F. Lin, Z.-Y. Huang, H.-W. Lin, P.-H. Wang, Y.-H.
1603 Liu, K.-T. Wong, J. Wen, D. J. Miller, S. B. Darling, *J. Am. Chem. Soc.* **2012**, *134*,
1604 13616.

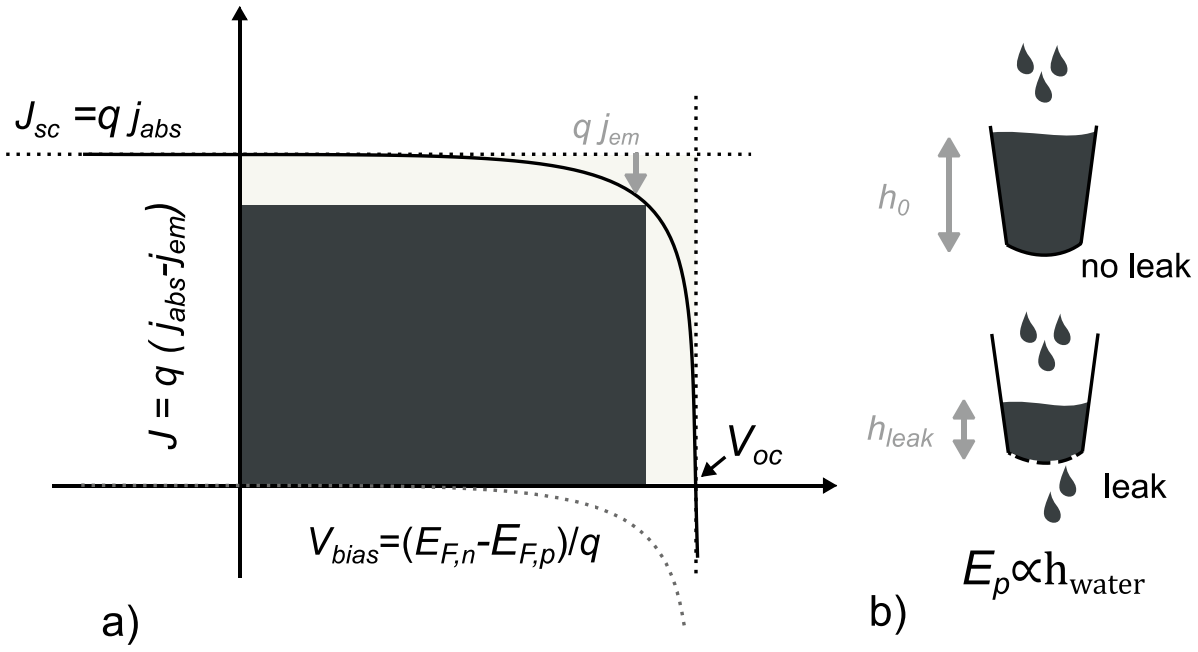

1605

1606

1607**Figure 1**: a) Schematic illustration of a *JV curve* for an ideal solar cell as derived from
1608thermodynamics and indicating the relevant parameters. The voltage corresponds to the quasi-

Fermi level splitting  , the difference between electron quasi-Fermi level E_{Fn} and the hole quasi-Fermi level  . The extracted current corresponds to the photons not re-emitted to the light source. The light grey arrow represents what is not extracted but lost due to emission. The ratio of the dark grey square, defined by the maximum power point and representing the maximum area under the JV curve, and the light grey square defined by V_{oc} and J_{sc}, is the 'Fill Factor' *FF*. At negative *J* values (injection), photons are emitted from the device, which corresponds to an LED. Adapted with permission from ref. [3] (copyright 2014, Springer Nature) . b) A 'leaky bucket' is a good analogy for recombination in a solar cell. The water level *h* (number of charge carriers) corresponds to the stored potential energy (chemical energy) and depends on how leaky (loss via recombination) the bucket is.

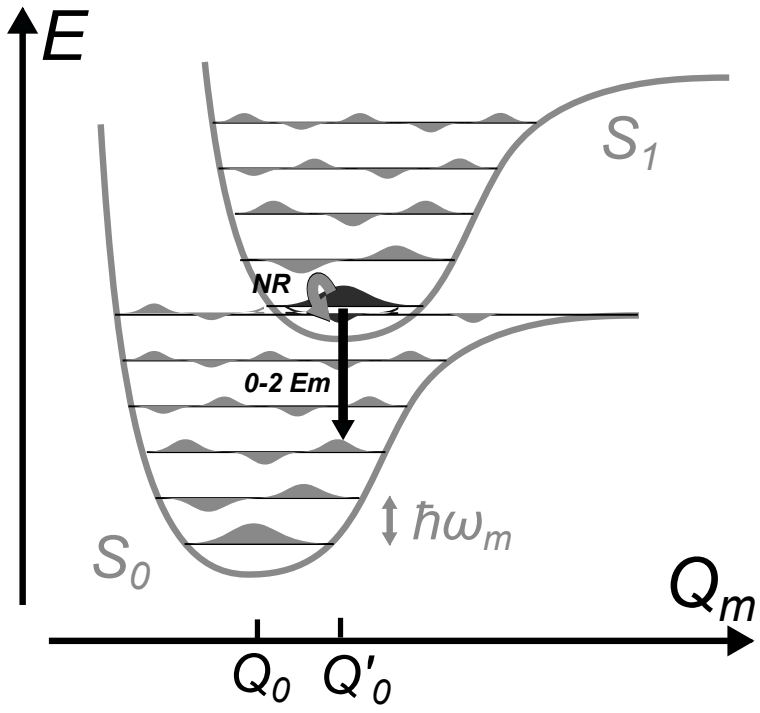

Figure 2: Energetic potential with respect to an effective nuclear coordinate Q_m for two different electronic energy levels. Grey areas represent the nuclear wavefunction amplitudes, which spread out with increasing energies within the slightly anharmonic potential. Because energy must be conserved, a very small overlap (shaded black) between the nuclear wavefunctions of the two electronic energy levels is obtained, resulting in a very low non-radiative transition probability. The curved and downward arrows indicate the non-radiative transition (NR) and the emission from S_1 (0^{th} vibrational level) to S_0 (2^{nd} vibrational level), respectively, which both occur at fixed Q_m.

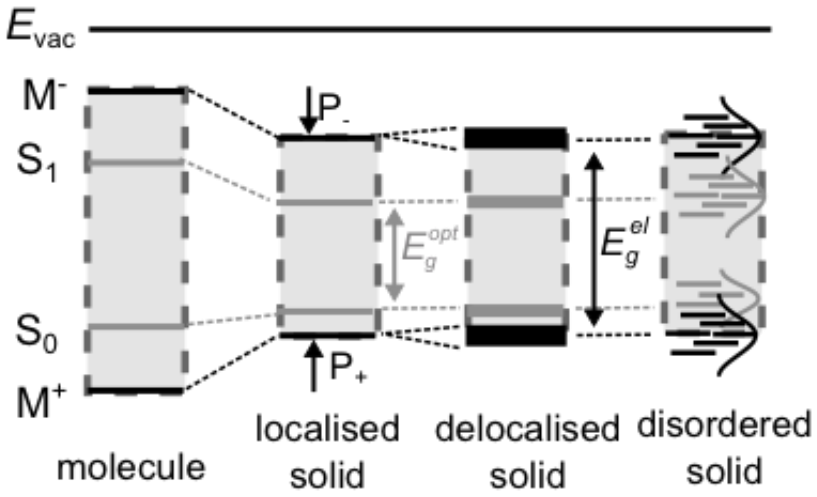

Figure 3 Changes in energy levels of neutral excited states (*excitons*, grey) and ionised excited states (*electrons and holes*, black) when going from individual molecules to a disordered solid. The polarisation energies $P_{+,-}$ correspond to partial screening of charges in the solid, which stabilises the *h* and *e* levels (EA and IP) with respect to the energies of the isolated molecule ($M^{+,-}$). This reduces the electrical gap E_g^{el}. The optical gap E_g^{opt}, defined by the S_0-S_1 transition is also reduced in the solid, as is the excitons binding energy E_g^{el}- E_g^{opt}. A high delocalisation increases the bandwidths of the excitonic and charge carrier levels, further decreasing the binding energy. Disorder, which is significant in organic semi-conductor films strongly localises charges and excitons. Adapted with permission from reference [3] (copyright 2014, Springer Nature).

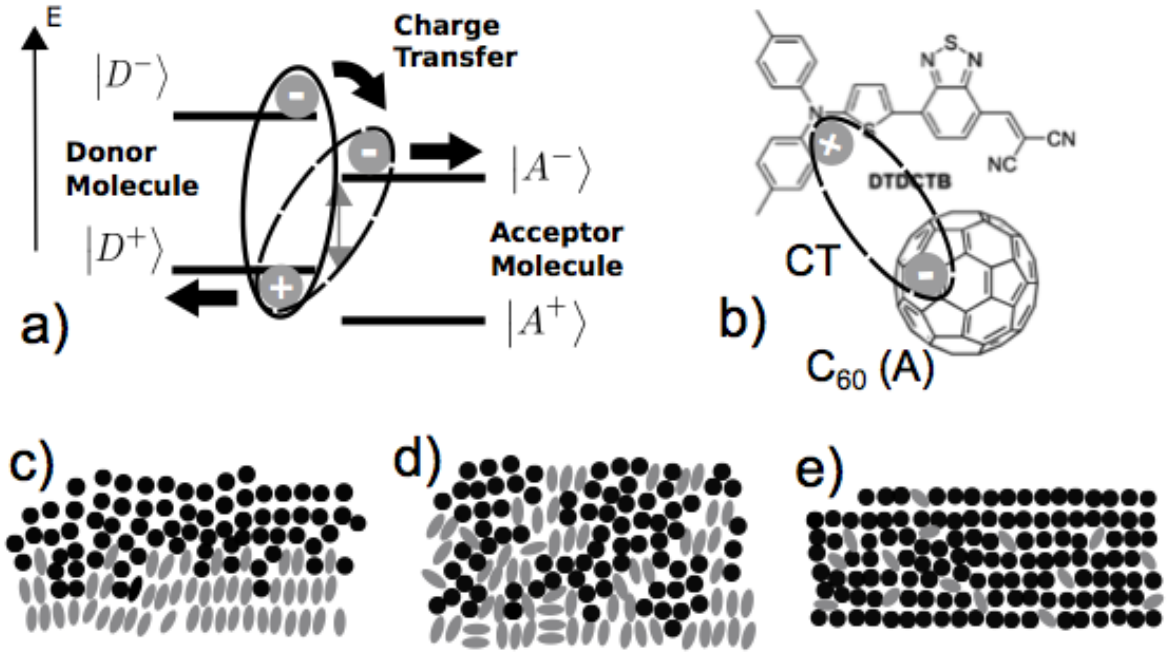

1644

1645

1646**Figure 4** Schematic illustrations of a) charge separation at a donor-acceptor (D-A)

1647heterojunction (HJ).It provides a simple introductory picture of the processes at the HJ, but is

1648physically unrepresentative and misleading (adapted with permission from ref. [24], copyright

16492009, Accounts of Chemical Research). In this schematic, the grey arrow corresponds to the

1650new electrical gap ϵ_r. b) a D-A charge transfer (CT) state formed between the small

1651molecule acceptor C_{60} and a push-pull donor, DTDTB[211], c) a planar D-A heterojunction

1652(PHJ) in which D (grey disks) and A (black circles representing fullerenes) are sequentially

1653deposited, note that the junction is deliberately not perfectly planar since there is always some

1654roughness and intermixing,[129] d) a 'bulk heterojunction' (BHJ) blend of D and A and e) a

1655'dilute' HJ with 95% fullerene acceptor.

1656

1657

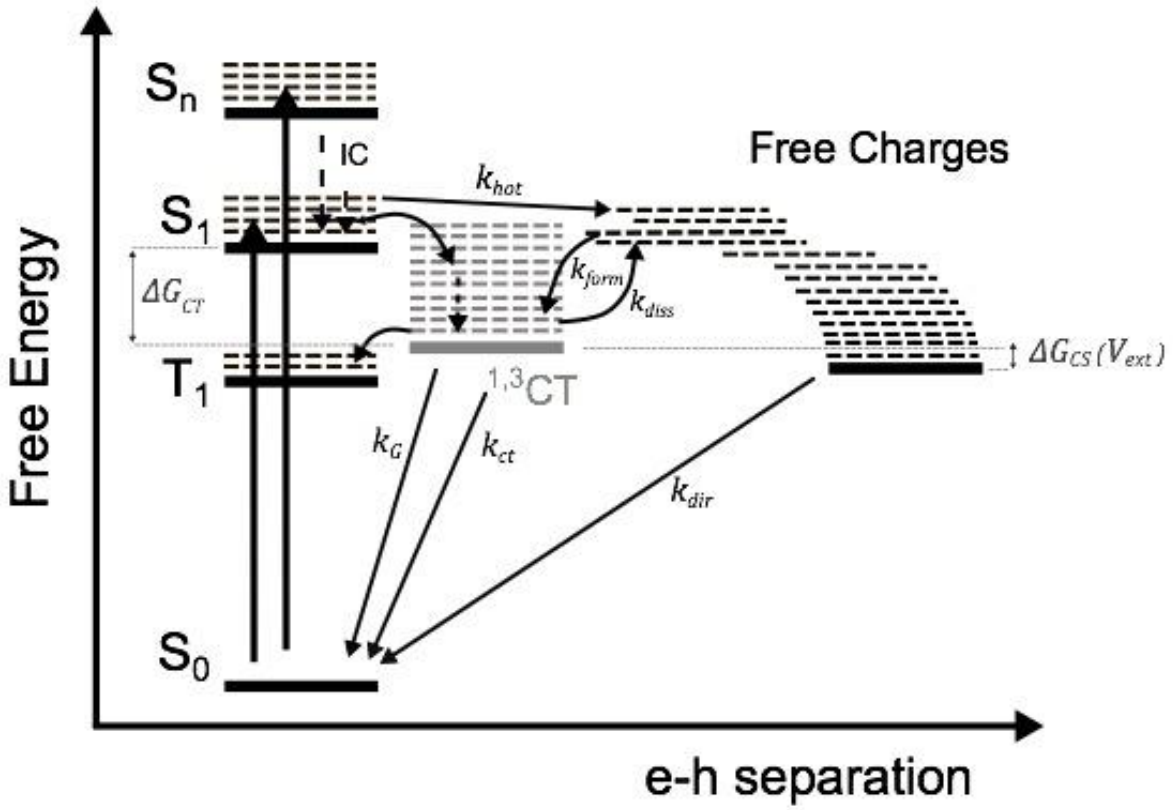

Figure 5. Jablonski diagram of charge separation and recombination processes in an organic solar cell. Solid vertical arrows correspond to allowed transitions and dashed downward arrows to internal conversion. Solid lines to S_0 represent recombination pathways. After absorption, charge transfer occurs resulting either in relaxed ^1CT states (curved + dashed arrows) or directly in free charges ( ). Free charges can recombine into CT states with rate ΔG_{CS}, from which they can recombine to the ground state with rate E_{ct}, or re-dissociate ($\Delta G_{CT}=E_{g,opt}-E_b$. ΔG_{CS} obeys spin statistics: 3/4 of events result in a triplet ^3CT, that can lead to triplet (T_1) back-formation. The key question is whether (relaxed) CT excitons can re-dissociate, that is whether k_{diss} is significant compared to ΔG_{CT}. Recombination is geminate (k_{diss}) if the recombining species originate from the same photon and non-geminate otherwise. k_{ct} is the driving force for charge transfer (exciton dissociation), and k_{dir} is the driving force for charge separation (CT state dissociation), which depends on the external bias V_{ext}. Adapted with permission from ref. [24], copyright 2009, Accounts of Chemical Research.

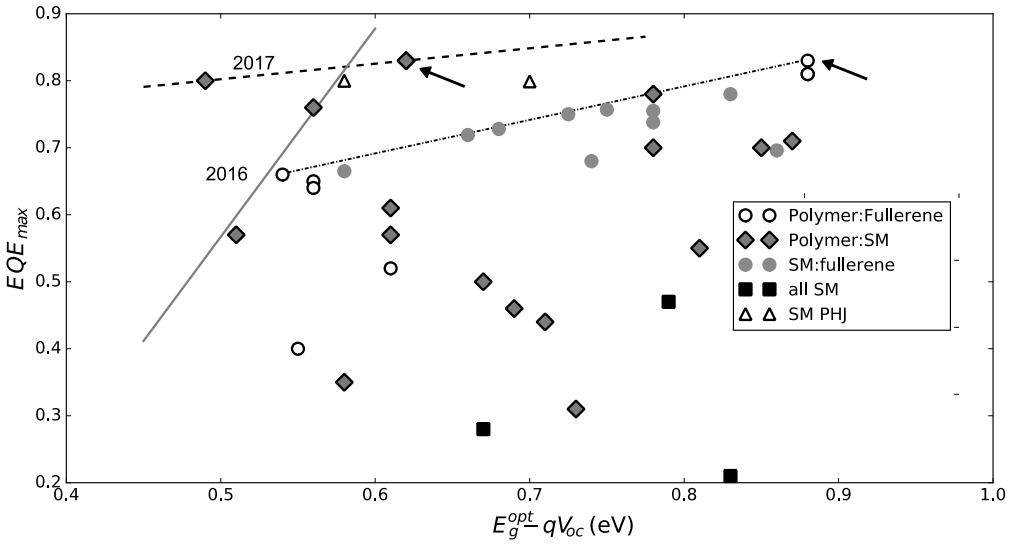
2017
2016
Polymer:Fullerene
Polymer:SM
SM:fullerene
all SM
SM PHJ
EQE_{max}
$E_g^{opt} - qV_{oc}$ (eV)

1672

Figure 6: Device data from literature illustrating the charge generation-V_{oc} trade-off, where EQE_{max} is used as proxy for the generation efficiency. The dashed and dashed-dotted grey line illustrate what we believe to be the magnitude of the trade-off at present for non-fullerene and fullerene acceptors respectively. The arrows indicate the champion NFA and fullerene devices. The solid grey line is drawn with the best results from 2016 and illustrates how rapidly NFA performance has risen.

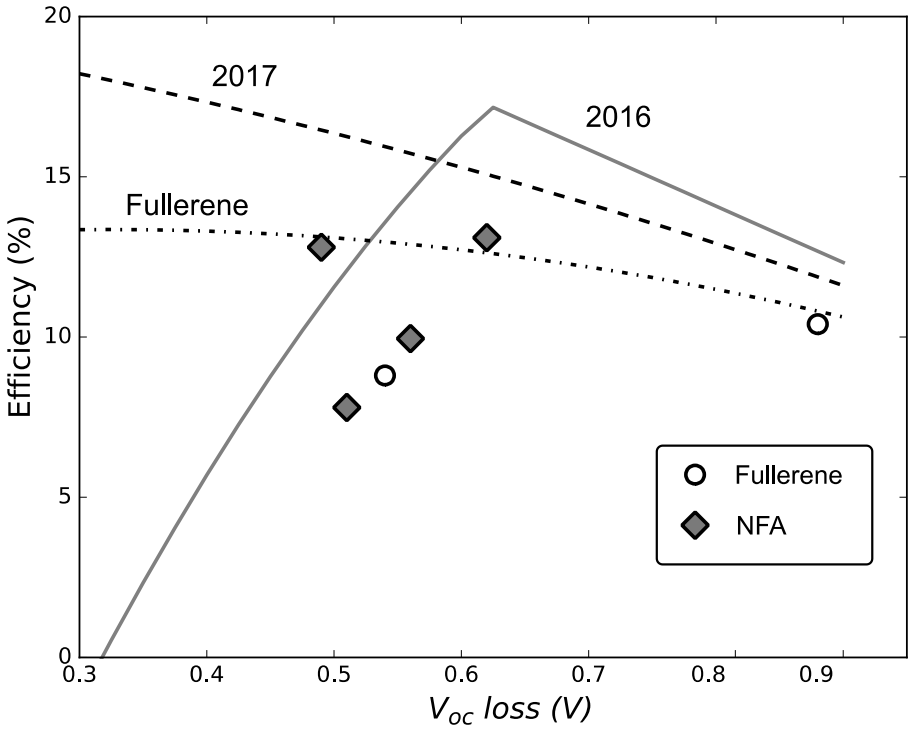

Figure 7: Simple estimates of the achievable OPV efficiencies for various generation-V_{oc} trade-off. The key assumptions are $EQE(h\nu) = EQE_{max}$ and E_g^{opt}=1.6eV. The *EQE* is capped to 0.95 and *FF* set at 0.75 (PCE calculation and data for *FF* 0.7 and 0.8 in Figure S1). Moving upwards corresponds to decreasing the *FF-absorption* trade-off, moving left to a reduced loss and shifting lines to mitigating the trade-off. The lines correspond to the *EQE*-V_{oc} trade-off guidelines of **figure 6** with $EQE(h\nu) = EQE_{max}$. The data points are also selected from **figure 6** and are, for NFAs, those along the dashed line,[187,201] and for fullerenes the champion device and the low loss system by Kawashima *et al.* that the dash-dotted line ends on.[1,40] NFAs beyond the dash-dotted line already outperform the empirical maximum achievable for fullerenes. Note that the data points have E_g^{opt} =1.5-1.65 eV while the simulation is performed for 1.6 eV.

Table 1: Vibrations deduced from (EL or PL) emission spectra and reference value for C_{60}.

Material [ref.]	E_g or E_{ct} /eV	$\hbar\omega_m$ /meV	EQE_{EL}
PffBT4T-2D:FBR [164]	1.6	131	1E-4
PffBT4T-2D:IDTBR [164]	1.6	-	3E-5
P3TEA: SF-PDI_2 [119]	1.72	167	5E-5
C_{60} [9] (CT)*	N/A	160	~1E-6
Rubrene:C_{60} [59] (CT)	1.46	160 (150) **	-
ITIC [194] (PL)	1.59	149	-

* From ΔV_{nr}. From absorption of the BHJ, which may overestimate the spacing. Emission from ref. [194] on ITIC also suggests a low vibrational energy but the emission is broad and more difficult to fit. ** Franck-Condon fit obtained in this work. The sample size is necessarily small since few works have reported emission spectra and EQE_{EL}s.

Author Biographies

Ivan Ramirez obtained his MSci in theoretical physics from Imperial College London in 2013. He then joined the Riede group in the Physics Department of the University of Oxford where he was the first student and helped build the experimental physics laboratory there. His research interests include the photo-stability and photo-physics of C_{60} and more recently V_{oc} losses. He has finished his PhD and recently joined Heliatek GmbH in Dresden, Germany.

Natalie Banerji is currently a Full Professor of Chemistry at the University of Bern. Her research interests include the study of organic and hybrid materials using ultrafast spectroscopic techniques, in view of solar cell and bioelectronic applications. She studied

Chemistry at the University of Geneva and obtained her Ph.D. in Physical Chemistry in 2009, under the supervision of Prof. Eric Vauthey. She then moved to the University of California in Santa Barbara (USA), to work on organic solar cells during a post-doctoral stay with Nobel Laureate Prof. Alan J. Heeger (2009-2011). In 2011, she started her independent research career in Switzerland at the Ecole Polytechnique Férérale de Lausanne (EPFL) with an Ambizione Fellowship by the Swiss National Science Foundation (SNSF). She moved to the University of Fribourg in 2014, was subsequently nominated Associate Professor in 2015, and presided the Chemistry Department in Fribourg form 2016-2017.

Moritz Riede is currently Associate Professor for Soft Functional Nanomaterials in the Department of Physics at the University of Oxford, UK. Before moving to Oxford in 2013, he worked in Germany at the Fraunhofer Institute for Solar Energy Systems ISE and the University of Freiburg as a PhD student (2002-2006), as well as at the Technische Universität Dresden as PostDoc and head of a junior research group (2007-2013) with Prof Karl Leo. In 2010 Moritz spent six months as visiting scholar at Stanford University, USA, and was visiting professor at the University of British Columbia, Canada, for three months in 2016. His academic research is focused on vacuum processed organic solar cells that have potential to transform the way we use solar energy.

1731**Table of Contents Entry**

1732

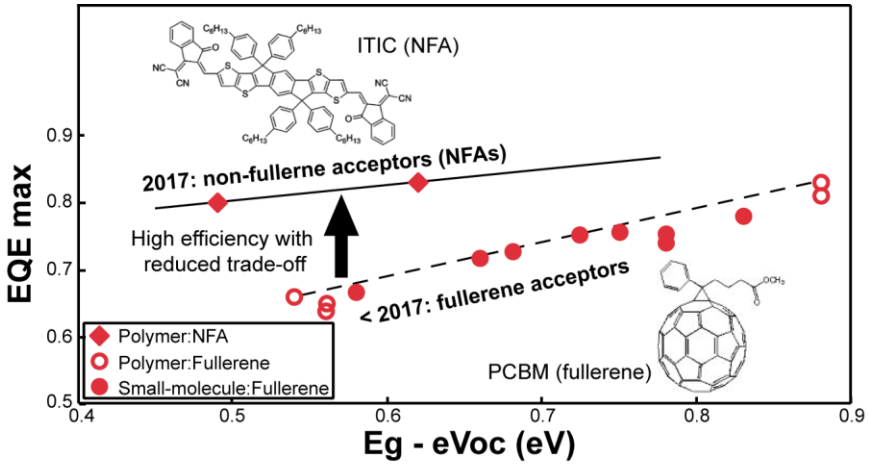

Organic photovoltaics have made astounding progress both in fundamental understanding and device performance. In particular non-fullerene acceptors (NFAs) bring into question previous empirical estimates of the achievable power conversion efficiencies. This report aims to provide a perspective on the physics underlying the conventional and new systems and their performance limits.

1733